904

LA-9484-PR

Progress Report

Los Alamos National Laboratory is operated by the University of California for the United States Department of Energy under contract W-7405-ENG-36.

Research and Development Related to the Nevada Nuclear Waste Storage Investigations

April 1—June 30, 1982

Los Alamos Los Alamos National Laboratory
Los Alamos, New Mexico 87545

The four most recent reports in this series, unclassified, are LA-8959-PR, LA-9095-PR, LA-9225-PR, and LA-9327-PR.

This report was prepared by the Los Alamos National Laboratory as part of the Nevada Nuclear Waste Storage Investigations managed by the Nevada Operations Office of the US Department of Energy. Based upon their applicability to the investigations, some results from the Radionuclide Migration Project, managed by the Nevada Operations Office of the US Department of Energy, are included in this report.

LA-9484-PR
Progress Report

UC-70
Issued: October 1982

Research and Development Related to the Nevada Nuclear Waste Storage Investigations

April 1—June 30, 1982

Compiled by
K. Wolfsberg
W. R. Daniels
B. R. Erdal
D. T. Vaniman

Contributors

R. D. Aguilar
B. H. Arney
W. S. Baldridge
B. P. Bayhurst
D. L. Bish
J. D. Blacic
D. E. Broxton
P. L. Bussolini
F. M. Byers
F. A. Caporuscio
B. M. Crowe
A. H. Davis
C. J. Duffy
S. D. Francis
R. R. Geoffrion
R. C. Gooley
G. H. Helken
L. E. Hersman
J. F. Kerrisk
F. L. Kerstiens
S. D. Knight
S. Levy
T. J. Merson
A. J. Mitchell
H. Nagel
D. C. Nelson
T. W. Newton
A. E. Norris
A. E. Ogard
N. A. Raybold
R. S. Rundberg
V. L. Rundberg
R. E. Semarge
W. L. Sibbitt
J. L. Thompson*
D. T. Vaniman
R. J. Vidale
P. L. Wanek

*Department of Chemistry, Idaho State University, Pocatello, ID 83209.

Los Alamos National Laboratory
Los Alamos, New Mexico 87545

CONTENTS

RESEARCH AND DEVELOPMENT RELATED TO THE NEVADA NUCLEAR WASTE STORAGE INVESTIGATIONS

April 1 - June 30, 1982

Compiled by

K. Wolfsberg, W. R. Daniels, B. R. Erdal, and D. T. Vaniman

Contributors

R. D. Aguilar
B. H. Arney
W. S. Baldridge
B. P. Bayhurst
D. L. Bish
J. D. Blacic
D. E. Broxton
P. L. Bussolini
F. M. Byers
F. A. Caporuscio
B. M. Crowe
A. H. Davis
C. J. Duffy
S. D. Francis
R. R. Geoffrion
R. C. Gooley
G. H. Heiken
L. E. Hersman
J. F. Kerrisk
F. L. Kerstiens
S. D. Knight
S. Levy
T. J. Merson
H. Nagel
D. C. Nelson
A. J. Mitchell
T. W. Newton
A. E. Norris
A. E. Ogard
N. A. Raybold
R. S. Rundberg
V. L. Rundberg
R. E. Semarge
W. L. Sibbitt
J. L. Thompson
D. T. Vaniman
R. J. Vidale
P. L. Wanek

ABSTRACT

This report summarizes the contribution of the Los Alamos National Laboratory to the Nevada Nuclear Waste Storage Investigations for the third quarter of FY 1982.

I. INTRODUCTION

This report summarizes some of the technical contributions from the Los Alamos National Laboratory to the Nevada Nuclear Waste Storage Investigations (NNWSI) project managed by the Nevada Operations Office of the US Department of Energy (DOE) during the period from April 1 through June 30, 1982. The report is not a detailed technical document but does indicate the status of some of the investigations being performed at Los Alamos.

II. FIELD MIGRATION EXPERIMENTS

A. Field Site (A. E. Norris, B. M. Crowe, and T. J. Merson)

The feasibility of constructing an adit near the Yucca Mountain exploration block is being investigated. The proposed adit is relatively shallow (~200 ft), but it would permit the performance of field experiments in tuff that is both unsaturated and similar to the geologic material in the exploraton block. Six outcroppings of tuff were surveyed to select a possible site for the adit. Four of the outcroppings exposed the Topopah Spring Member, and the remainder exposed bedded tuffs of Calico Hills. One of the four Topopah Spring Member sites was selected for detailed surveying and horizontal coring. The first draft of criteria for the horizontal coring was prepared. Analyses of the cores will provide data for the next step in the site selection process for this adit.

The most promising site for an adit in the bedded tuffs of Calico Hills is located in the Prow Pass area. The outcropping is outside the current US Air Force use-permit area. The area has been found to contain archeological ruins. The time required to renegotiate the use permit and to prepare and implement an archeological impact mitigation plan is estimated to be at least 6 months. A delay of this length would affect adversely the timeliness of data for the Yucca Mountain repository horizon selection process.

The Grouse Canyon tuff in G-Tunnel was inspected this quarter as a potential site for a radionuclide migration field experiment, should the adit in the unsaturated tuff prove to be infeasible for this work.

An investigation has been initiated to determine the status of engineering test equipment and designs available at Lawrence Livermore National Laboratory and Sandia National Laboratories for conducting radionuclide migration studies in the field.

B. Development and Characterization of Groundwater Tracers (P. L. Wanek)

Additional preliminary investigations were made to separate and detect salts of fluorinated benzoic acids by high-performance liquid chromatography (HPLC). Sodium salt solutions were made of six fluorinated benzoic acids (o-fluorobenzoic acid, m-fluorobenzoic acid, p-fluorobenzoic acid, pentafluorobenzoic acid, α,α,α-trifluoro-m-toluic acid, and α,α,α-trifluoro-o-toluic acid) by adding an equivalent amount of 0.01 M NaOH to a weighed portion of acid to achieve an approximate final concentration of 800 to 850 mg salt/ℓ. (This assumes a yield of 1 meq salt/meq base added. Because no titration of the salt was made, concentrations of salts were estimated from weights.) Ultraviolet spectra of the salt solutions were obtained in an attempt to determine the optimum wavelength for monitoring HPLC separations. A wavelength that would provide strong absorbance for all compounds of interest, yet be free of interferences from matrix components, etc., would be advantageous.

The salts were run individually by HPLC, using a C18 column and a mobile phase mixture of methanol, water, and phosphate buffer (pH 5.5) prepared by adding 0.1 M K_2HPO_4 (initial pH 9.2) to a 0.1 M solution of KH_2PO_4 (initial pH 4.48) to achieve a final solution with the desired pH of 5.5. A wavelength of 225 nm was chosen to monitor the HPLC relation. Individual retention times for the salts were obtained; then separation of a mixture of all six salts plus a "parent" salt of commercially prepared, nonfluorinated sodium benzoate was attempted. Unfortunately, under the conditions used, two of the salts had nearly identical retention times and were not adequately resolved from the component mixture. The retention times of the individual salts do not seem to correlate with the measured pK_a values,[1] nor are they necessarily expected to.

Ultraviolet spectra were obtained for solutions of nitrate, nitrite, and water from well J-13. Nitrate species were reported to interfere with detection of the tracers,* and it was thought that components of well J-13 water might also interfere; therefore, a set of spectra of such background matrix components seemed advisable. The spectra indicated possible significant interference only in the wavelength region below 210 nm and probably only at low tracer concentrations.

*From information supplied to K. Wolfsberg by the Department of Hydrology, University of Arizona, Tucson, Arizona.

Further studies are planned to optimize the monitor wavelength, using a Spectra-Physics wavelength scanning program, and to determine sensitivity limits and matrix effects encountered in a field test.

III. GEOCHEMISTRY OF TUFF

A. Groundwater Chemistry (A. E. Ogard, R. A. Aguilar, B. P. Bayhurst, A. J. Mitchell, and P. L. Wanek)

Water samples from wells USW-H3 and USW-H4 at Yucca Mountain have been chemically analyzed.

Well USW-H3 was not producing a sufficient amount of water and was not pumped. Therefore, the samples for analysis were taken by swabbing prior to the injection testing of the well. The high chloride content (35 mg/ℓ), high lithium content (2.6 mg/ℓ), and the high detergent content of the water, all of which were introduced during the drilling, indicate that analyses of samples from unpumped wells have no geochemical value. The high content of suspended $Fe(OH)_3$ and black rubber particles in the water shows also that swab samples are not usable samples. The $Fe(OH)_3$ is known to be a good adsorber and precipitating agent for other cations.

Well USW-H4, however, was pumped for ~9 days; the results of analyses of water at the end of the pumping period are given in Table I. Each sample was anaerobically collected, filtered through a 0.05-μm Nuclepore membrane, and then sent to Los Alamos for chemical analysis. The electrode measurements were made in the field. These results must be used with caution. Although the pumping duration was 9 days, the water exiting the pump continued to foam; obviously the water still contained detergent from the drilling of the well and was not pure formation water. After the pump had been stopped and removed from the well, at-depth samples were taken at selected intervals using evacuated stainless steel bottles. The analytical results on these samples, when completed, will serve as baseline compositions for any further pumping and analyses of the water from this well.

A program for the testing of a single stratum of well UE25b-1 was set up and implementation started in June. Of primary concern in the determination of the chemistry of the groundwater is knowing when the water is formation water, free from any of the drilling fluids. The main components of fluids used in the drilling of hydrology wells are well J-13 water, air, and detergent. Lithium chloride is also added to serve as a tracer for the water used as drilling fluid.

TABLE I

COMPOSITION OF GROUNDWATER FROM WELL H-4

Analyses by PES[a]		Analyses by IC[b]	
Element	Concentration (mg/ℓ)	Anion	Concentration (mg/ℓ)
Mg	0.194	F^-	4.5
Mn	0.005	Cl^-	6.2
Si	25.9	NO_2^-	c
Fe	0.031	PO_4^{3-}	c
Sr	0.017	NO_3^-	4.7
Ba	0.003	SO_4^{2-}	23.9
V	0.008		
Ti	0.031	Electrode Data	
Ca	10.8	pH = 7.4	
Li	0.156	Eh = +250 mV	
K	2.65	$[O_2]$ = 5.8 mg/ℓ	
Al	0.045	$[S^{2-}] < 10^{-9}$ M	
Na	84.2		

[a] Plasma emission spectroscopy.

[b] Ion Chromatography.

[c] Not detected.

It is especially important to eliminate all drilling fluids because the oxygen concentration of the groundwater is one of the most important variables in the chemistry of the water, affecting retardation mechanisms and corrosion of the waste package. Winograd and Robertson[2] have suggested that groundwaters in the tuffs of Nevada may always contain dissolved oxygen. It seems reasonable that the flowing water that may be the least influenced by oxygenated recharge water and by air in the unsaturated tuffs or fractured tuffs will be the water in the deepest permeable zone.

The deepest permeable zone in well UE25b-1 was determined previously by "tracejector" tests to be at 2840 to 2870 ft.* This zone is separated from other permeable zones above it by ~200 ft of more impermeable tuff; therefore, we plan to try to isolate this permeable zone with a bridge plug at 3000 ft and a packer at 2800 ft. The water from between these packers will be pumped at a constant rate of ~200 gal./minute until we have indications that we have achieved formation water (maximum of 30 days at this time).

Periodically samples will be taken anaerobically and analyzed. The Eh, pH, oxygen concentration, sulfide concentration, and temperature of the water will be measured several times a day using electrodes. Analyses of samples will be made daily in the field for anion constituents, and acid-stabilized, anaerobically filtered (0.05-μm) samples will be sent back to Los Alamos for cation analysis. Field analysis will also be made on the detergent content of the water to determine if the sulfonate ion in the detergent can be used as a measure of how well the water is being cleared of drilling fluids.

B. Solubility of Plutonium(IV) in Natural Waters with Carbonate Present

(J. F. Kerrisk)

1. Introduction. In natural waters that are not strongly oxidizing, soluble plutonium generally exists as Pu(IV). The solubility of Pu(IV) will depend on the activities of many of the species in the water. The influence of carbonate on Pu(IV) solubility is of particular interest here. Thermodynamic data exist for only one complex of Pu^{4+} with CO_3^{2-},

$$Pu^{4+} + CO_3^{2-} = PuCO_3^{2+} \quad . \qquad (1)$$

*Data supplied by the Nuclear Hydrology Group, US Geological Survey, Denver, Colorado.

These data are based on the experiments of Moskvin and Gel'man (hereafter referred to as MG), who measured the solubility of Pu(IV) in carbonate solutions in contact with $Pu(OH)_4(s)$.[3] The MG experiments were recently reviewed by Lemire and Tremaine,[4] who estimated $\log_{10} K_1 \leq 41$; K_1 is the equilibrium constant for Eq. (1),

$$\frac{[PuCO_3^{2+}]}{[Pu^{4+}]\ [CO_3^{2-}]} = K_1 \quad ,$$

where square brackets indicate activity. In the EQ3/6 chemical-equilibrium computer program,[5] the data base has $\log_{10} K_1 = 40.7$ at 25°C.

The influence of K_1 on plutonium solubility can be seen from calculations of plutonium solubility in water that is typical of Well J-13 at Yucca Mountain.[6] Table II shows the composition of the water. The total carbonate content of the water is 2.9×10^{-3} molal. Calculations of uranium and plutonium solubility as a function of solution Eh and pH were done with the EQ3 program.[5] Both uranium and plutonium were assumed to be present. Figure 1 shows plutonium solubility (solid lines) and Fig. 2 shows uranium solubilty (solid lines) as a function of pH at four values of Eh that range from strongly oxidizing to reducing conditions (700, 400, 100, and -200 mV). At pH <7, the plutonium solubility equals the carbonate content of the water (Fig. 1). Under these conditions, essentially all the plutonium and carbonate exist as the $PuCO_3^{2+}$ complex. This is directly attributable to the stability of this complex, which is implicit in $\log_{10} K_1 = 40.7$. At high pH values, the plutonium solubility is below the total carbonate content, but it is still quite high because of the $PuCO_3^{2+}$ complex (Fig. 1).

If the value of $\log_{10} K_1$ is as large as 40, this has significant implications for the waste disposal program. However, the experimental results of MG have been criticized as indicating that $PuCO_3^{2+}$ is much too stable.[7] MG also measured formation constants for plutonium-oxalate complexes at the same time as the $PuCO_3^{2+}$ formation constant; their oxalate data are in agreement with other measurements indicating their technique was valid for the oxalate complexes.[7]

2. Moskvin and Gel'man Experiments. The MG experiments involved measurements of total plutonium in solutions in contact wth $Pu(OH)_4(s)$; the solutions had various carbonate concentrations from 0.36 to 3.6 M (Ref. 3). Two groups of experiments were done. In the first, seven measurements were reported where

TABLE II

WELL J-13 WATER[a]

Element or Species	Total Concentration (molal)
Na	2.0×10^{-3}
K	1.4×10^{-4}
Ca	2.9×10^{-4}
Mg	7.1×10^{-5}
Al	9.6×10^{-7}
Si	1.1×10^{-3}
Sr	4.6×10^{-7}
Ba	1.7×10^{-8}
Mn	2.0×10^{-8}
Fe	7.9×10^{-7}
V	6.3×10^{-7}
F	1.1×10^{-4}
Cl	1.8×10^{-4} [b]
(PO_4^{3-})	1.0×10^{-6}
(NO_3^-)	1.6×10^{-4}
(SO_4^{2-})	1.9×10^{-4}
(CO_3^{2-})	2.9×10^{-3}

[a] pH = 6.9. Ti (6×10^{-7} molal) and Li (1×10^{-5} molal) are not included in the calculations because they are not available in EQ3.

[b] Amount adjusted to obtain electrical neutrality.

the ionic strength was controlled (at ~7 and ~10 M) and the pH was held at 11.5. The total plutonium in solution increased with increasing carbonate content. In the second group of experiments, no attempt was made to control the ionic strength and the pH varied from 9.7 to 11.6. For 7 measurements the total

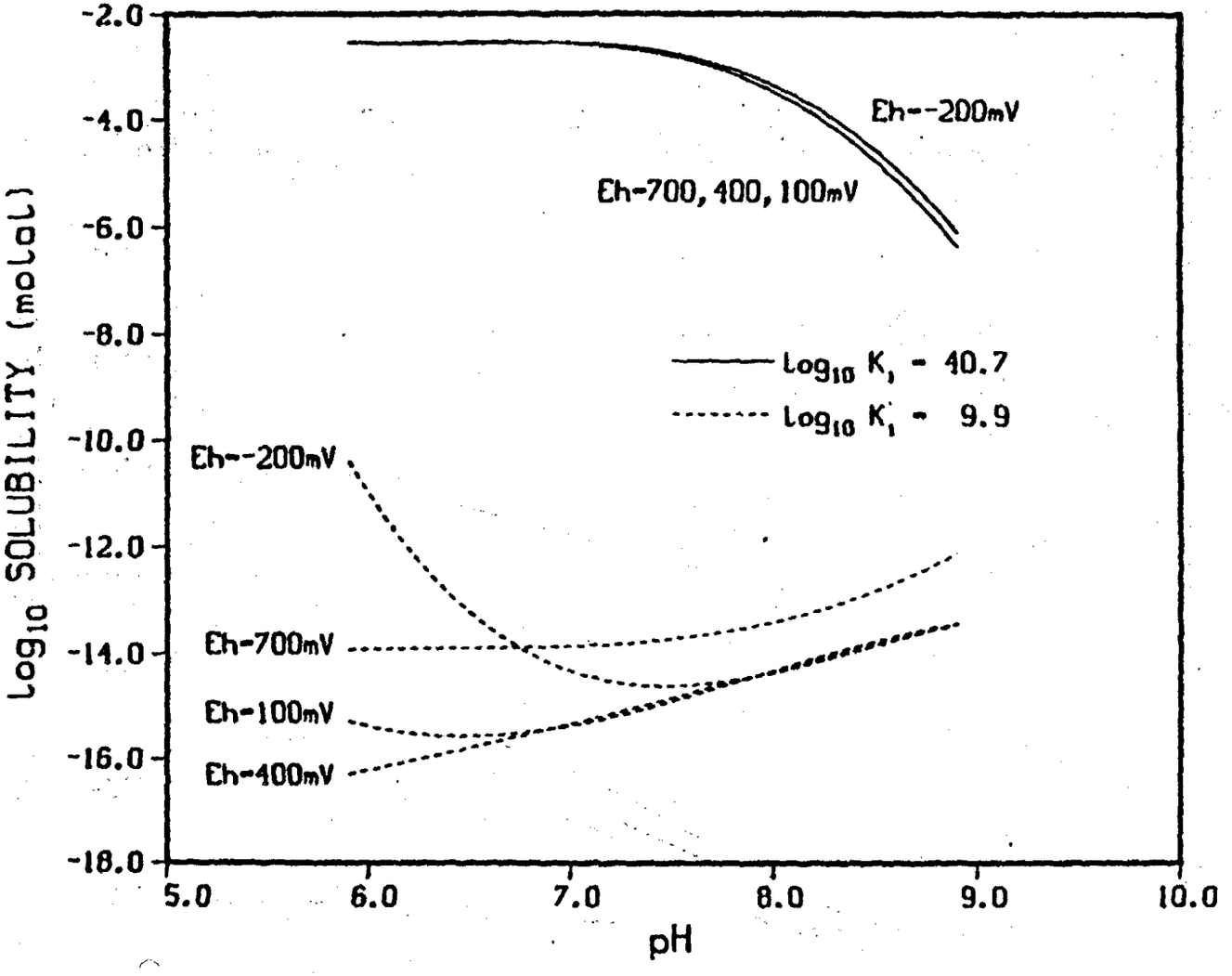

Fig. 1. Plutonium solubility in well J-13 water.

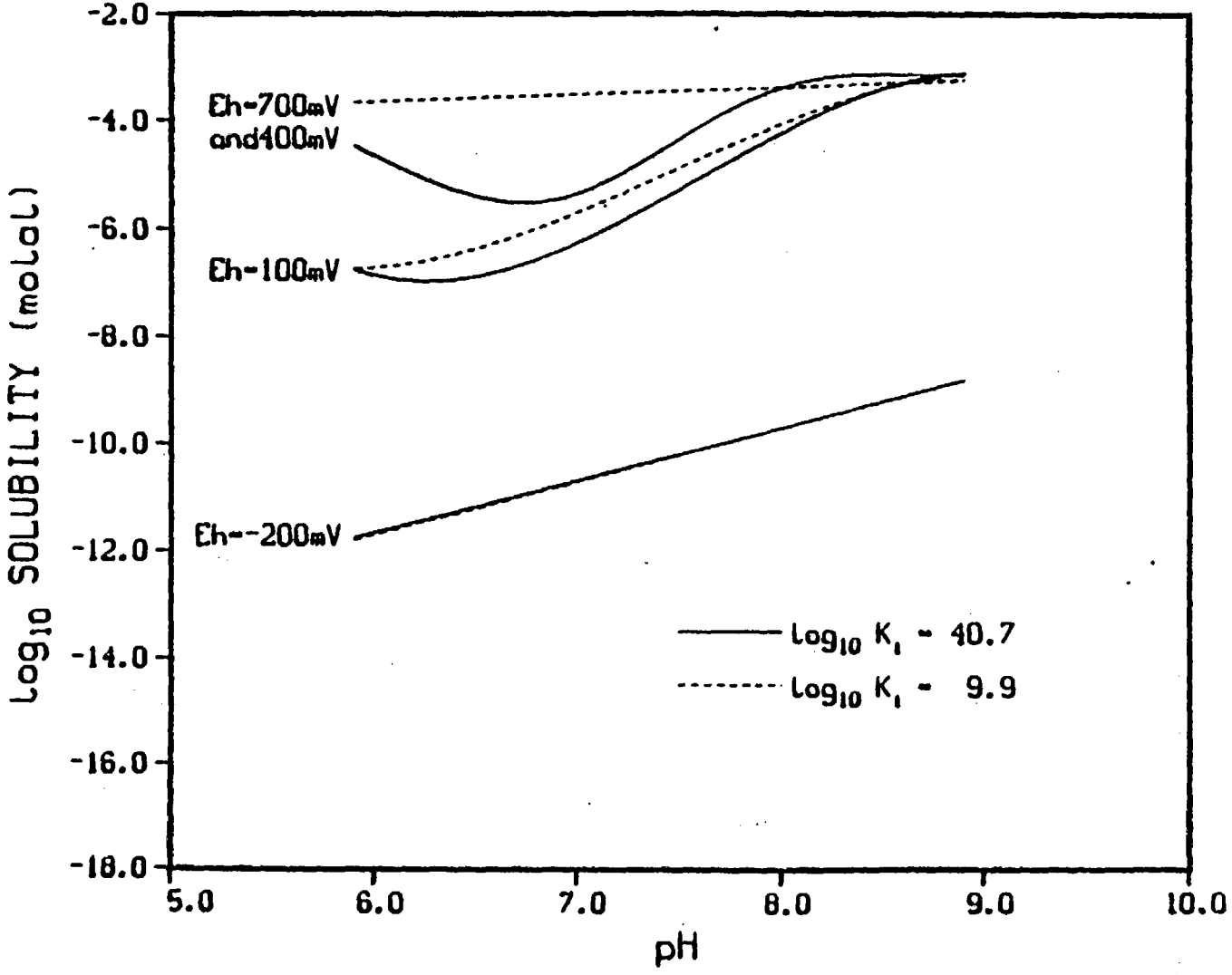

Fig. 2. Uranium solubility in well J-13 water.

plutonium concentration first increased and then decreased with increasing carbonate content. From these measurements, MG reported $\log_{10} K_1 \cong 47$. Lemire and Tremaine have recently reviewed the MG experiments.[4] Using revised data for the solubility of plutonium in contact with $Pu(OH)_4(s)$, they estimated $\log_{10} K_1 \leq 41$.

In analyzing their data, MG assumed that all the soluble plutonium was tied up in a single carbonate complex. Their data indicated a plutonium-to-carbonate ratio of 1, thus giving the $PuCO_3^{2+}$ complex. To assess this assumption and others inherent in the MG experiments, calculations of the solubility of plutonium under the conditions of the MG experiments were done with the EQ3 program.[5] Only one Pu(IV) complex with carbonate is in the EQ3 data base, $PuCO_3^{2+}$, with $\log_{10} K_1 = 40.7$. Table III shows results from this calculation for the controlled ionic strength experiments. The calculations were done for a solution Eh = 400 mV; the solution ionic strength was maintained at the experimental value by addition of potassium chloride. The calculated plutonium solubility is well above the measured results at the lower carbonate concentrations, but is in general agreement for the other cases. In addition to total calculated plutonium solubility, Table III also shows the concentrations of the two major aqueous plutonium species, $Pu(OH)_5^-$ and $PuCO_3^{2+}$. It is evident that the $Pu(OH)_5^-$ concentration is a factor of 10 to 100 greater than the $PuCO_3^{2+}$ concentration. Thus, one of the primary assumptions used by MG to calculate K_1 appears to be invalid. The high ionic strength of the solutions used by MG means that EQ3 is well outside the range where accurate activity coefficients are calculated.[8] For this reason, the EQ3 results must be considered approximate.

Table IV shows results from EQ3 calculations for the second group of experiments, in which the ionic strength was not controlled. Besides the varying ionic strength, the pH also varied among these experiments. Some difficulties were encountered in the calculation for the lowest carbonate (and lowest pH) case; a very large plutonium solubility (~1 M) was indicated by results that did not converge. At the two lowest values of pH (9.7 and 10.6), the calculated plutonium solubility is much greater than the experimental results. Most of the aqueous plutonium is as $PuCO_3^{2+}$ at pH <11.25 because the Pu^{4+} concentration increases rapidly as the pH drops. This occurs because the Pu^{4+} concentration and OH^- concentration are related through the solubility of $Pu(OH)_4(s)$,

$$[Pu^{4+}]\ [OH^-]^4 = K_{sp} \quad ,$$

TABLE III

EVALUATION OF $PuCO_3^{2+}$ FORMATION CONSTANT EXPERIMENTS - CONTROLLED IONIC STRENGTH[a]

Experimental[b]			EQ3 Results with $\log_{10} K_1 = 40.7$			EQ3 Results with $\log_{10} K_1 = 9.9$		
Total Carbonate Content (M)	Plutonium Solubility (M)	Ionic Strength (molal)	Plutonium Solubility (molal)	Concentration (molal)		Plutonium Solubility (molal)	Concentration (molal)	
				$PuCO_3^{2+}$	$Pu(OH)_5^-$		$PuCO_3^{2+}$	$Pu(OH)_5^-$
0.362	1.78×10^{-4}	7.0	1.40×10^{-3}	2.82×10^{-5}	1.37×10^{-3}	1.37×10^{-3}	4×10^{-35}	1.37×10^{-3}
0.724	2.58×10^{-4}	7.0	1.51×10^{-3}	4.37×10^{-5}	1.46×10^{-3}	1.46×10^{-3}	6×10^{-35}	1.46×10^{-3}
1.448	5.79×10^{-4}	7.0	1.69×10^{-3}	5.69×10^{-5}	1.63×10^{-3}	1.63×10^{-3}	8×10^{-35}	1.63×10^{-3}
2.172	1.15×10^{-3}	10.0	1.31×10^{-3}	9.82×10^{-5}	1.21×10^{-3}	1.22×10^{-3}	1×10^{-34}	1.21×10^{-3}
2.896	1.28×10^{-3}	10.0	1.42×10^{-3}	9.13×10^{-5}	1.32×10^{-3}	1.33×10^{-3}	1×10^{-34}	1.32×10^{-3}
3.216	1.44×10^{-3}	10.0	1.47×10^{-3}	8.86×10^{-5}	1.37×10^{-3}	1.38×10^{-3}	1×10^{-34}	1.37×10^{-3}
3.62	1.65×10^{-3}	10.8[c]	1.40×10^{-3}	9.42×10^{-5}	1.30×10^{-3}	1.30×10^{-3}	1×10^{-34}	1.30×10^{-3}

[a] pH = 11.5.

[b] Reference 3.

[c] Concentration of K_2CO_3 brought ionic strength >10.

TABLE IV

EVALUATION OF $PuCO_3^{2+}$ FORMATION CONSTANT EXPERIMENTS - IONIC STRENGTH NOT CONTROLLED

Experimental[b]				EQ3 Results with $\log_{10} K_1 = 40.7$			EQ3 Results with $\log_{10} K_1 = 9.9$		
Total Carbonate Content (M)	pH	Plutonium Solubility (M)	Ionic Strength (molal)	Plutonium Solubility (molal)	Concentration (molal)		Plutonium Solubility (molal)	Concentration (molal)	
					$PuCO_3^{2+}$	$Pu(OH)_5^-$		$PuCO_3^{2+}$	$Pu(OH)_5^-$
0.724	9.7	1.66×10^{-4}	--	large[b]	--	--	4.16×10^{-5}	3×10^{-29}	4.15×10^{-5}
1.448	10.6	5.4×10^{-4}	3.9	1.32×10^{-1}	1.32×10^{-1}	2.90×10^{-4}	2.85×10^{-4}	2×10^{-32}	2.85×10^{-4}
2.172	11.4	1.34×10^{-3}	6.5	1.64×10^{-3}	1.44×10^{-4}	1.49×10^{-3}	1.49×10^{-3}	2×10^{-35}	1.49×10^{-3}
2.536	11.2	1.2×10^{-2}	7.5	1.92×10^{-3}	1.05×10^{-3}	8.63×10^{-4}	8.66×10^{-4}	2×10^{-34}	8.63×10^{-4}
2.896	11.2	7.11×10^{-3}	8.6	1.64×10^{-3}	7.54×10^{-4}	8.83×10^{-4}	8.87×10^{-4}	1×10^{-34}	8.83×10^{-4}
3.26	11.4	6.59×10^{-3}	9.7	1.35×10^{-3}	2.13×10^{-4}	1.13×10^{-3}	1.14×10^{-3}	3×10^{-35}	1.13×10^{-3}
3.62	11.6	1.67×10^{-3}	10.8	1.68×10^{-3}	3.76×10^{-5}	1.63×10^{-3}	1.64×10^{-3}	5×10^{-36}	1.63×10^{-3}

[a] Reference 3.

[b] Calculation did not converge; plutonium solubility ~1 molal.

where K_{sp} is the $Pu(OH)_4(s)$ solubility product constant. For the other five cases, the calculated plutonium solubility ranges from 1.3×10^{-3} to 1.9×10^{-3} molal; the measured plutonium solubility ranges from 1.3×10^{-3} to 12×10^{-3} M. The experimental results do not correlate well with total carbonate content or pH. The calculated results are primarily a function of pH and secondarily a function of carbonate content and ionic strength. As with the constant-ionic-strength group of experiments, the EQ3 calculations for this group indicate that a significant amount of the aqueous plutonium exists as $Pu(OH)_5^-$, particularly at higher values of pH. Thus, these calculations also indicate that one of the primary assumptions employed by MG may not be valid.

The fact that most of the soluble plutonium is tied up as $Pu(OH)_5^-$ under the conditions of the MG experiments indicates that their calculation would overestimate the stability constant of $PuCO_3^{2+}$ (their estimate of $\log_{10} K_1$ would be too large). This conclusion is the same as the previously referenced criticism of the MG experiment.[7] Because of this potential problem with the formation constant of $PuCO_3^{2+}$, an independent estimate of K_1 is pursued in the next section.

3. An Independent Estimate of K_1. Although experimental thermodynamic data are preferable to data estimates, data estimation techniques are often useful for testing the consistency of groups of data for similar species. One technique that has been used with actinides is a plot of formation constants for various aqueous complexes as a function of the number of ligands in the complex.[9] Figure 3 shows such a plot for complexes of U^{4+}, Th^{4+}, and Pu^{4+} with ligands OH^-, HPO_4^{2-}, SO_4^{2-}, F^-, and CO_3^{2-} (Refs. 4,9,10). The quantity β_n is the equilibrium constant for the reaction,

$$M + nL = ML_n \quad ;$$

that is,

$$\frac{[ML_n]}{[M]\,[L]^n} = \beta_n \quad ,$$

where M is a metal ion and L is a ligand. The only carbonate data shown are for $PuCO_3^{2+}$ (derived from the MG results) and for $U(CO_3)_5^{6-}$. The inconsistency of the $PuCO_3^{2+}$ data ($\log_{10} K_1 = \log_{10} \beta_1 = 40.7$) with all the other data is evident from this plot. If it is assumed that U^{4+} and Pu^{4+} form carbonate complexes of similar stability, the $U(CO_3)_5^{6-}$ result (n = 5) can be extrapolated,

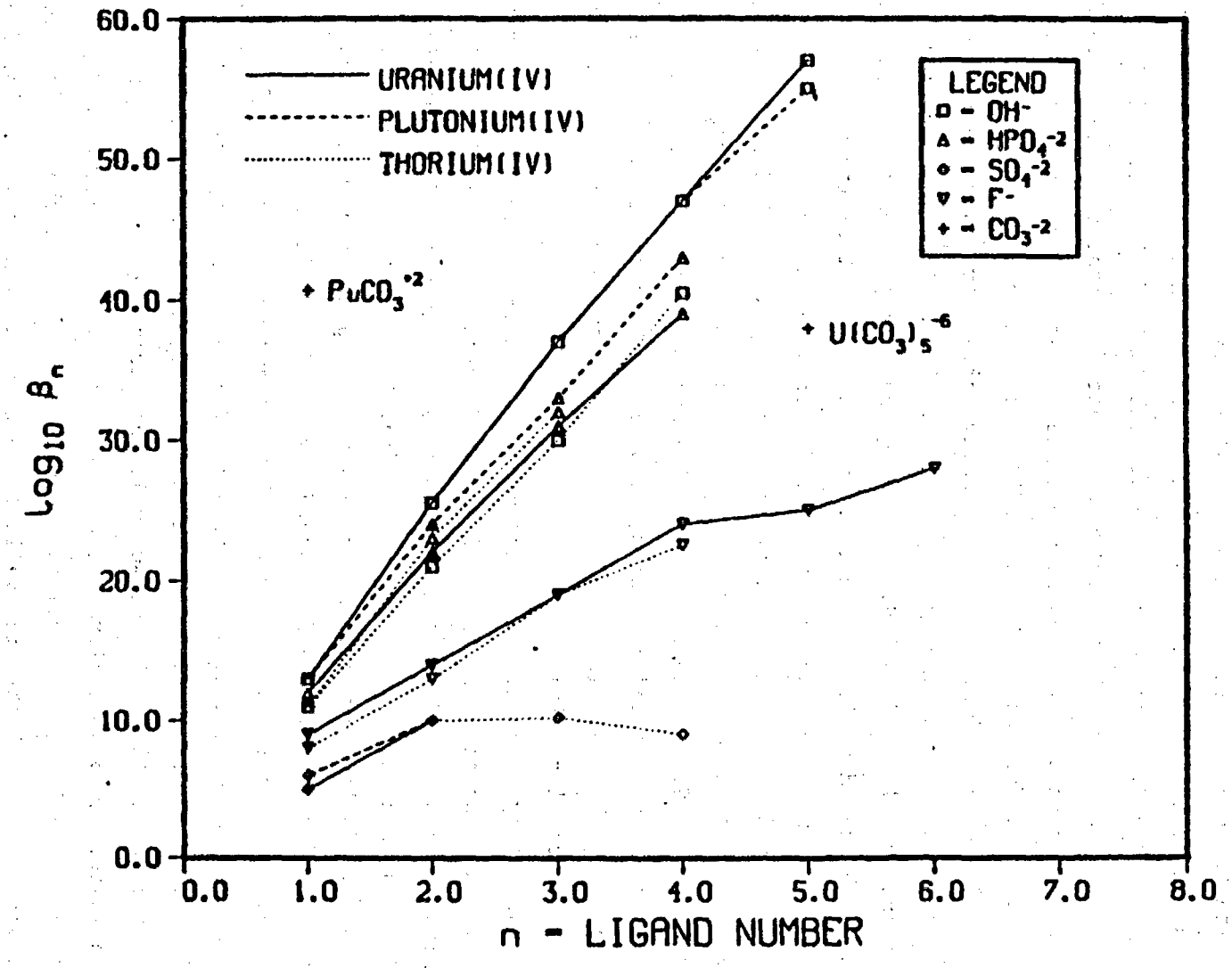

Fig. 3. Formation constants for aqueous actinide species.

parallel to the lines for the other ligands, to n = 1 (Ref. 7). This gives $\log_{10} K_1 \cong 10$ as an estimate of the formation constant of $PuCO_3^{2+}$ that is consistent with the other actinide aqueous-complex data.

Calculations for the conditions of the MG experiments were rerun with EQ3 using $\log_{10} K_1 = 9.9$. These results are also shown in Tables III and IV for the experiments with and without controlled ionic strength, respectively. For the controlled ionic strength cases, where the pH was also controlled at 11.5, there is little difference between the calculated plutonium solubility with $\log_{10} K_1 = 40.7$ or 9.9 (Table III). Plutonium solubility under these conditions is mostly accounted for by the $Pu(OH)_5^-$ complex. The $PuCO_3^{2+}$ concentration is insignificant when $\log_{10} K_1 = 9.9$. For the group of experiments in which the ionic strength and pH varied (Table IV), the plutonium solubility is also relatively independent of the magnitude of K_1 for high pH (pH $\geq$11.4). At lower pH, the calculated plutonium solubilities using $\log_{10} K_1 = 9.9$ are more in line with the experimental solubilities. Thus, for most of the experimental conditions employed by MG, the choice between 40.7 and 9.9 for $\log_{10} K_1$ makes little difference in the calculated plutonium solubility. When there is a significant difference, $\log_{10} K_1 = 9.9$ gives better agreement between calculated solubility and the experimental results.

The solubility of uranium and plutonium in Well J-13 water was also recalculated with EQ3, using $\log_{10} K_1 = 9.9$ as the formation constant for $PuCO_3^{2+}$. The results are shown in Figs. 1 and 2 as the dashed curves. The plutonium solubility has been reduced substantially (Fig. 1). For the calculations where $\log_{10} K_1 = 40.7$ (solid curves), the primary aqueous plutonium species was $PuCO_3^{2+}$ in all cases. For the calculations where $\log_{10} K_1 = 9.9$ (dashed curves), the primary aqueous plutonium species varies with Eh and pH, being PuO_2^+, $PuO_2CO_3^{2-}$, $Pu(OH)_5^-$, or Pu^{3+} under different conditions. The solubility of uranium in Well J-13 water is influenced by the choice of $\log_{10} K_1$ (Fig. 2). Under oxidizing conditions (Eh = 700 and 400 mV), when uranium(VI) is the primary oxidation state, aqueous complexes between UO_2^{2+} and CO_3^{2-} can form. For the calculations where $\log_{10} K_1 = 40.7$ (solid curves), all the carbonate is tied up with plutonium so that little is available to complex with uranium. For the calculations when $\log_{10} K_1 = 9.9$ (dashed curves), the higher CO_3^{2-} concentration increases the concentration of uranium(VI)-carbonate complexes and thus increases the solubility of uranium. Under reducing conditions (Eh = -200 mV), uranium exists primarily as uranium(IV). No complexes of uranium(IV) with carbonate are

available in the EQ3 data base (either they are not stable or thermodynamic data are unavailable), so the uranium solubility is unaffected by changes in $\log_{10} K_1$ (Refs. 4 and 5).

4. Conclusions. The objective of this analysis was to assess the effect of carbonate on the solubility of plutonium, particularly Pu(IV). It became obvious after some initial calculations that the stabilty of the $PuCO_3^{2+}$ complex, as indicated by the work of MG, would dominate plutonium solubility whenever carbonate is present. However, the MG data have been criticized as indicating that $PuCO_3^{2+}$ is much too stable. The value for the formation constant based on their work ($\log_{10} K_1 = 40.7$) is not consistent with other actinide aqueous-complex data; a value of $\log_{10} K_1 \cong 10$ is more in line with other actinides.

The EQ3 computer program was used to calculate plutonium solubility under the conditions of the MG experiments. Although these calculations must be considered approximate because of the high ionic strengths involved, they indicate that one of the major assumptions used to analyze the MG data, that $PuCO_3^{2+}$ is the primary aqueous plutonium species under the experimental conditions, is not valid. Because of the high pH employed in these tests, $Pu(OH)_5^-$ is the primary aqueous species under most conditions. The plutonium-oxalate complex measurements made by MG were at very low pH (pH ≅1), where hydroxyl complexes would be insignificant.

The plutonium solubilities calculated by EQ3 using $\log_{10} K_1 = 9.9$ are in better agreement with the measured results than are the calculated solubilities using $\log_{10} K_1 = 40.7$. However, the agreement is far from good. There are a number of possible reasons for the differences.

(1) Inaccurate activity coefficients caused by the high ionic strengths may contribute to disagreements. An examination of Table III shows that plutonium solubilities are affected by the change in ionic strength from 7 to 10.

(2) Inaccurate thermodynamic data for aqueous complexes in EQ3 may also lead to some disagreements. The EQ3 data base is probably the best available at this time, but inaccurate formation constants or missing data for some complexes are still possibilities. The formation constant for the complex $Pu(OH)_5^-$, which is important under these experimental conditions, is consistent with formation constants for other actinide hydroxyl complexes (Fig. 3).

(3) Uncertainties in the experimental conditions may also result in disagreements. The EQ3 calculations indicate that plutonium solubility is a strong function of pH under the conditions of the MG experiments. Also, solution Eh was not reported. Calculations were done at Eh = 400 mV; at higher Eh, Pu(VI) and its aqueous complexes become important, increasing the solubility of plutonium. Plutonium solubility was unaffected by decreasing the solution Eh below 400 mV.

The primary conclusion of this analysis is that the potential importance of Pu(IV)-carbonate complexes and the uncertainty in their thermodynamic data warrant an experimental investigation of this system. Carbonate is an important complexing agent in essentially all natural waters; thus, plutonium-carbonate complexes must be considered at all repository sites, not just at Yucca Mountain.

C. Plutonium Chemistry in Near-Neutral Solutions (T. W. Newton and V. L. Rundberg)

Plutonium(IV) polymer is of environmental importance because it may provide a mechanism for transport, either directly or by adsorption onto fine particles that may be transported. Conversely, large polymer particles would be expected to be filtered out by the geologic media, and adsorption onto immobile phases would contribute to retardation. For these reasons we are continuing our work on polymeric forms of plutonium.

We showed in an earlier report that when Pu(IV) in acid solution is diluted so as to give plutonium concentrations near 3×10^{-6} M and a pH of ~3, all the species capable of rapid reaction with Os(II) complexes disappear within 1 or 2 hours. It was concluded that most of the product of this reaction is Pu(IV) polymer because very little (~10%) Pu(III) and/or Pu(V) was found using Ce(IV) as the reagent.

We have now repeated these experiments at higher concentrations to decrease analytical difficulties, and we find that approximately half the initial Pu(IV) is converted to Pu(III) and Pu(V). A solution 1.2×10^{-5} M in total plutonium was prepared in 10^{-3} M acid, and aliquots were treated periodically with either Ce(IV) sulfate or $Os(dimebipy)_3^{2+}$. After 3 minutes, reaction with Os(II) showed that ~60% of the original Pu(IV) remained. After 330 minutes, essentially all the Pu(IV) had disappeared. After 340 minutes, reaction with Ce(IV) showed that ~45% of the original Pu(IV) had been converted to Pu(III) and/or Pu(V). This

is consistent with approximately equal rates for disproportionation and for polymerization under the conditions of the experiment. The overall rate of disappearance of Pu(IV) observed is in agreement with the results reported in an earlier report.[11] The effects of pH and plutonium concentration on the relative rates of disproportionation and polymerization have yet to be determined.

The precipitation and adsorption properties of diluted Pu(IV) prepared as described above may be important in the environment; therefore, they were investigated in preliminary experiments.

The Pu(IV) solution was diluted to 6.2×10^{-6} M in 0.001 M acid and the pH was then adjusted to 5.1 by the addition of a 1 M pyridine solution. This base was used because it forms a buffer that is useful for pH values between 4.5 and 6 and it does not appear to complex plutonium in this range.

Centrifugation for 4 hours at 12 000 rpm (28 000 g) or filtration through a 0.4-μm Nuclepore filter removed 57 ± 10% or 64 ± 7% of the plutonium, respectively. More plutonium was removed by filtering the supernatant from centrifugation through a 0.05-μm membrane; after this treatment only 19% of the original plutonium remained dissolved or suspended.

Adsorption onto Pyrex was observed. This material was ground, sieved to give particles in the range from 106 to 150 μm, washed with hydrochloric acid, and thoroughly rinsed with water. Ratios of weight of solid to volume of solution ranged from 0.56 to 5.11 mg/mℓ. After 3 days of contact, about two-thirds of the plutonium in a 6×10^{-6} M solution at pH 5.1 was adsorbed onto the largest glass sample. The distribution ratio showed no trend with amount of glass and averaged 0.41 mℓ/mg with a mean deviation of 0.08 for four determinations.

This adsorption is irreversible in the sense that only ~2% of the plutonium was removed by stirring for 2 hours in 0.001 M acid and only 5% in 0.01 M acid.

Similar experiments, also at pH 5, using two forms of silica, 9-μm powder and diatomaceous earth, showed that ~60% of the plutonium was adsorbed in 30 minutes, independent of the amount or type of silica used. The ratios of solid to liquid were in the range from 0.6 to 2.9 mg/mℓ.

Further experiments will involve longer contact times, other solids, and attempts to characterize the nonadsorbed material with respect to filterability and the presence of reducing species [Pu(III) and Pu(V)].

Precipitation and adsorption experiments were also done using green polymer prepared at a concentration of 8×10^{-3} M in ~0.04 M hydrochloric acid. Polymer prepared in this way is easily characterized by its optical absorption

spectrum. A polymer suspension was diluted to 6×10^{-7} M total plutonium at a pH of ~5; it was found that ~96% of the plutonium could be removed either by centrifugation for 3 hours at 12 000 rpm or by filtration through 0.4-μm Nuclepore membrane. This result indicates that the solubility of the polymer is $<2.4 \times 10^{-8}$ M. Rai and Swanson[12] report a solubility of 5×10^{-7} M at pH 5; they do suggest, however, that most of their soluble material was in the form of Pu(V) rather than Pu(IV), although the oxidizing agent was not identified. They also report that solubility equilibrium was reached in ~8 days. The apparent solubility of our polymer was found to increase slightly with time. After 45 days in contact with air, the concentration of plutonium that remained after centrifugation had doubled.

In another experiment we used 3×10^{-6} M total plutonium at a pH of 4.5 and found that only ~13% of the plutonium could be removed by centrifugation at 12 000 rpm for 2.5 hours. This suggests a strong dependence of solubility on pH. Further experiments will be required before we will understand the apparent discrepancies between our results and those reported by Rai and Swanson.

The effect of HCO_3^- on the precipitation of polymer was observed in a single exploratory experiment. In 0.5 M NH_4HCO_3, only ~27% of the plutonium in a 6×10^{-6} M suspension was removed by centrifugation at 12 000 rpm for 2 hours. This is a larger "solubility" than might be expected and might be due to carbonate complexing or to the adsorption of carbon dioxide by the polymer, as has been reported.[13]

Adsorption of the green polymer onto SiO_2 and ground Pyrex was briefly investigated at a pH of 4.6. The amount of plutonium adsorbed from 3×10^{-6} M solutions during a 1000-minute contact period was found to be independent of the solid-to-liquid ratio in the range from 0.5 to 2.7 mg/mℓ. The amount of plutonium adsorbed was 94% for the SiO_2 and 83% for the Pyrex. Further work at lower concentrations will be required before this adsorption behavior can be explained.

D. Particulate Transport (J. L. Thompson)

Most studies concerning the transport of radioactive material away from a repository have assumed that the waste form dissolves, then moves as ions in solution. An alternate mode of transport involves the radioactive material moving as a particulate suspension in the groundwater. Particles of colloidal size (~1 to 10^{-3} μm in diameter) may remain suspended for very long periods of time and, hence, migrate at the rate of groundwater flow. The radioactive particles may form by leaching of the solid-waste form, by sorption of dissolved

radionuclides on nonradioactive particles, or by formation of colloids by radioactive species (for example, actinide hydrous oxides).

Various mechanisms may act to remove particulates from groundwater. Mechanical filtration will remove larger particles. Particles may sorb on the surface of rock pores, held there by van der Waals forces. The presence of ions in solution, particularly multivalent ions, may neutralize the electrostatic repulsive charges on the colloids, allowing them to coagulate.

We have initiated studies of particulate transport as it may occur in tuff derived from the Nevada Test Site (NTS). Our first work has involved determining some limiting parameters that control the mechanical aspects of this phenomenon. For this purpose we have used commercially manufactured polystyrene beads and fluorescent resins not soluble in water. In later experiments we will use colloidal material more like that which may be encountered in a repository environment.

A fluorescent resin was obtained from the Day-Glow Color Corporation, Cleveland, Ohio. This material was a mechanically ground powder with a wide range of particle sizes. Filtration of water suspensions through 0.4- and 0.05-μm Nuclepore membranes separated the smaller particles for subsequent use. Suspensions of these small (<0.05-μm diam) particles were stable over periods of several days, with no evident settling. Several qualitative experiments were performed with these Day-Glow suspensions. It was observed that the suspension readily passed through a crushed-rock column containing G1-1883 tuff rock fragments in the size range of 106- to 250-μm diameter. Similarly, the suspension was drawn through an intact disc of G1-2840 tuff 0.70 mm thick. A fluorometer is on order, and when it arrives we will be able to quantify losses of the particulate resin during passage through crushed rock or solid rock.

Polystyrene microspheres with nominal diameters of 3 and 9 μm were obtained from the 3M Company, St. Paul, Minnesota. Some of the 9-μm microspheres were labeled with ^{85}Sr. The nonlabeled microspheres were readily observable with an optical microscope. The 9-μm spheres were remarkably uniform in size, but the 3-μm spheres included an appreciable fraction of smaller spheres that appeared to range in size down to ~1 μm. It was found that some of the 9-μm microspheres could be carried through the crushed-rock column by rinse water flowing under the force of gravity. Most of the spheres were retained by the column. Of these, many were not stopped by purely mechanical trapping because when the column was rinsed with ethyl alcohol a large number of the spheres were eluted. Attempts to observe passage of the microspheres, including those down

to 1 μm in size, through the tuff disc were unsuccessful. Neither repeated water nor alcohol rinses seemed to carry any spheres through the solid-rock matrix. Experiments are now underway to study particle transport along fractures in solid-rock cores.

E. Phase Change Studies (C. J. Duffy)

Experiments have been started that examine the phase changes in tuffs of varying mineral composition at known values of pressure and temperature. The samples are ground and enclosed in gold capsules with water present. The capsules are then placed in standard cold-seal pressure vessels that are pressurized and heated to the desired conditions. In these experiments water pressure is equal to the total pressure. Table V shows the mineral compositions of the starting materials and the compositions of final products after 2 weeks at 400°C and 400 bars and after 4 weeks at 300°C and 400 bars.

The experiments are preliminary, but they do illustrate several interesting points. The upper stability limit of mordenite is apparently below 400°C at 400 bars in most of these rocks; however, in sample BH, a tuff from Buckhorn, New Mexico, mordenite is apparently stable at 400°C. Two explanations are possible. The mordenite may be metastable at 400°C; this seems unlikely because clinoptilolite in the other runs at 400°C did not produce mordenite. More likely, the stability of mordenite in this sample is due to a difference in composition. Such a difference might be in the ratio of potassium to sodium. There is also some indication that the mordenite in these samples is stable above 300°C. In those samples that originally contained clinoptilolite and mordenite, mordenite has crystallized at the expense of clinoptilolite. This is, however, not definitive evidence of mordenite stability. Mordenite may well be a metastable product of clinoptilolite decomposition. Certainly this is the case for cristobalite, which is known to be metastable with respect to quartz under these conditions. The observation of mordenite growth at the expense of clinoptilolite also indicates that the upper temperature stability limit of clinoptilolite is <300°C at 400 bars water pressure. Sample G2-547 indicates that this may also be true for montmorillonite.

Fifteen-week runs were completed at 200°C and 400 bars, but no change was observed in any of the samples. In samples G1-1319 and G2-547, where glass and feldspar are present, the lack of change is certainly due to the slowness of the kinetics. In the remainder of the samples the mineral assemblages present may be stable under these conditions. Larger quantities of the materials are

TABLE V

MINERAL COMPOSITIONS OF STARTING MATERIAL AND HYDROTHERMAL RUN PRODUCTS AT 400 BARS WATER PRESSURE[a]

Sample	Starting Composition	Run at 300°C	Run at 400°C
BH	clinoptilolite	clinoptilolite	mordenite cristobalite?
G1-1319	glass feldspar cristobalite?	glass feldspar cristobalite?	feldspar glass cristobalite?
G1-1639	clinoptilolite minor mordenite	clinoptilolite mordenite cristobalite feldspar?	Feldspar cristobalite
G2-547	feldspar montmorillonite	feldspar montmorillonite?	feldspar cristobalite
G2-762	clinoptilolite minor cristobalite	clinoptilolite cristobalite	feldspar cristobalite minor quartz
G2-2001	mordenite clinoptilolite	mordenite minor quartz cristobalite?	feldspar cristobalite minor quartz
G2-2667	mordenite quartz	mordenite quartz	feldspar quartz

[a]Minerals for each sample and experiment are listed in approximate order of abundance.

currently being run to produce material with which to reverse the reactions that have been observed.

Preliminary hydrothermal experiments have provided evidence on the upper thermal stabilties of clinoptilolite and mordenite at 400 bars water pressure. The upper stability of mordenite is probably between 300 and 400°C, and that for clinoptilolite appears to be below 300°C. These conclusions are made somewhat uncertain by lack of knowledge of the exact compositions of the minerals and by questions of metastability.

Future work will attempt to reverse the reactions that have been observed and determine the bulk compositions of the starting materials.

F. Microbiological Activity at Yucca Mountain (L. E. Hersman)

Routine microbial analyses have been performed on the drilling polymer and soap currently in use at Yucca Mountain in the NTS. Initial results suggest that both substances can serve as growth substrates for microorganisms.

Soil samples were obtained at two drilling locations in Yucca Mountain. One location was receiving discharges of the polymer, and the other site was exposed to the soap. Two samples from each site were collected, placed in polypropylene bottles, stored at ambient temperature, and immediately returned to Los Alamos for analysis. Samples were collected from these areas because it was felt that such soils would be good sources of microorganisms capable of degrading soap and polymer.

Initial analysis consisted of transferring small amounts (1.0 g) of soil onto solid medium or into liquid medium. The ingredients listed in Table VI were used as a minimal-salts growth medium. Either 5 mℓ of polymer (diluted 2/42) or 5 mℓ of soap (diluted 1/50) were added to 1 ℓ of the minimal-salts medium. Solid medium was made by adding 15 g of agar to 1 ℓ of medium.

Because both media contained no nutrient energy source other than the soap or the polymer, any growth in these media can be interpreted as a direct use of these materials by the growing microorganisms. Some nutrient carryover could occur; that is, small amounts of nutrients from the soil could be transferred along with the microorganisms. To avoid that, additional transfers of the growing microorganisms are usually made, thereby diluting out any nutrient carry-over.

Preliminary results strongly suggest that both the soap and the polymer can serve as energy sources for soil microorganisms because luxuriant growth occurred in all the media. Upon closer microscopic examination, all media

TABLE VI

MEDIUM FOR GROWTH OF MICROORGANISMS[a]

Ingredient[b]	Quantity used in growth medium
$NaNO_3$	1.5 g
K_2HPO_4 (1.5)	5 mℓ
$MgSO_4 \cdot 7H_2O$ (1.5)	5 mℓ
Na_2CO_3 (0.8)	5 mℓ
$CaCl_2$ (0.5)	10 mℓ
$Na_2SiO_3 \cdot H_2O$ (1.2)	10 mℓ
citric acid (1.2)	1 mℓ
KH_2PO_4 (3.0)	5 mℓ
$FeSO_4 \cdot 7H_2O$	0.001 g
H_3BO_3	10 μg
$MnSO_4 \cdot H_2O$	10 μg
$ZnSO_4$	70 μg
$CuSO_4$	50 μg
MoO_3	10 μg
yeast extract	1 g
trace element solution	1 mℓ
H_2O	1 ℓ

[a]Medium has 7.2 pH.

[b]Numbers in parentheses indicate g/200 mℓ H_2O, used for stock solution.

contained mixed cultures of microorganisms, with many species being motile. Several colony shapes were present on the solid media, with many exhibiting significant mucoid excretions. These excretions are usually characteristic of known biodegraders, such as the pseudomonads. From the first set of solid nutrient media, several colonies were transferred to a second set of nutrient media. Here again vigorous growth occurred, and because no nutrient carry-over could be present after the transfer, it is assumed that the microorganisms were using both the soap and the polymer as energy sources.

These results demonstrate that there is strong potential for microbial activity in drilling fluids; however, it should be stressed that the effects

of such activity are, as yet, unknown. Because a growing microbial population can result in change in soil pH and Eh, microbial use of drilling fluids could affect radionuclide movement. In addition, many researchers strongly suspect that soil microorganisms provide chelating agents that also affect metal movement in soil systems.

G. Crushed-Rock Columns (R. S. Rundberg and N. Raybold)

All previously reported crushed-rock column experiments have been terminated and the results reported.[14] A new set of crushed-rock column experiments has been initiated; these columns are being run at higher flow rates than those heretofore. The flow rates have been chosen to minimize diffusion spreading and to observe peak spreading that could be attributed to mass transfer kinetics. The peak shapes will be compared with chromatography theory and other sorption models. Anionic tracers will be used with these columns to observe the anion exclusion effect produced by various mineral compositions.

The following crushed-rock columns have been prepared and correspond to whole-core columns that are being run concomitantly: G1-2698, G1-2233, G1-2334, G1-2840, G1-2410 (all 38- to 106-μm wet-sieved fractions), and G1-2854 (38- to 75-μm wet-sieved fraction). The densities and free column volumes of these columns have been determined, and the columns will now be spiked with $^{95}Tc^{m}$, ^{85}Sr, ^{137}Cs, and ^{133}Ba.

The sorption of TcO_4^- on the 106- to 150-μm fraction of crushed Climax Stock granite had been attributed[15] to the possible presence of hematite. The experiment has now been repeated using Climax Stock granite crushed in an agate ball mill. The sorption of TcO_4^- has not been observed in the latest experiment, and the previous results are now attributed to iron contamination.

H. Solid-Core Columns (R. S. Rundberg, A. J. Mitchell, and N. A. Raybold)

The following whole-core columns have been prepared and spiked with HTO: YM-54, G1-2854, G1-2289, G1-2840, G1-2334, and G1-2410. The dispersivities and kinetic void volumes will be determined. These columns will be spiked with $^{95}Tc^{m}$ to determine the effect of anion exclusion in solid-core columns. In addition, the columns will be spiked with ^{85}Sr, ^{137}Cs, and ^{133}Ba. Two columns of tuffs G1-2840 and G1-2334 have been prepared for use with a high-pressure metering pump. These columns will be used to observe transport at high fluid velocities to detect the effect of mass-transfer kinetics.

I. Dependence of the Sorption Ratio on Element Concentration (S. D. Knight and R. S. Rundberg)

It is important to determine the type of sorption isotherm for different elements on different tuff samples for diffusion and transport calculations.

Batch sorption measurements have been performed with a wet-sieved, 75- to 500-μm fraction of sample G1-2840, a devitrified tuff. Experiments performed with strontium and cesium have been completed. The results for strontium are listed in Table VII and the data for the cesium experiments are being processed.

Twelve solutions of different strontium concentrations traced with ^{85}Sr were prepared with rock-treated water that had been filtered through 0.05-μm Nuclepore membranes. The strontium concentrations were measured with a plasma-emission spectrometer and ranged from 8×10^{-7} to 10^{-3} M. Duplicate experiments were performed for 3 weeks at ambient temperature under atmospheric conditions. For the cesium experiments, 12 traced solutions of different concentrations were prepared by diluting a standard cesium solution and adding ^{137}Cs tracer. Cesium concentrations ranged from 10^{-9} to 10^{-3} M.

Sorption ratios remain practically constant for initial strontium concentrations between 10^{-7} and 10^{-5} M but tend to decrease with increasing concentration above 10^{-5} M. The strontium concentrations in solution (C) and on the solid (Q) after the contact time were determined for each sample; a log-log plot of these data is given in Fig. 4. The isotherm obtained is not linear, but the data fit a Langmuir isotherm. This information will be useful for modeling purposes.

J. Determinations of Anion Concentrations of Groundwater (P. L. Wanek)

A mobile laboratory was set up with equipment for groundwater chemical analyses. Because the Dionex ion chromatograph, which was used extensively for analyses of anions, was part of the instrumentation to be moved to the NTS, an alternate means of running anion analyses using the Spectrophysics HPLC instrument at Los Alamos was investigated. Experiments were run using a Vydac analytical anion column with a Wescan conductivity detector and phthalic acid eluent, and with the Dionex analytical column (no suppressor) and benzoic acid eluent. It was not possible to use the suppressor column, normally used on the Dionex instrument, on the Spectrophysics instrument. Fluoride could not be analyzed on the Vydac column. The Dionex column showed more promise, but further studies to determine detection limits, etc., must be done to establish whether that method

TABLE VII

VARIATION OF SORPTION RATIOS FOR G1-2840 TUFF WITH STRONTIUM CONCENTRATION

Initial Strontium Concentration (M)	R_d (mℓ/g)
1.42×10^{-3}	9.20
	9.72
8.49×10^{-4}	14.8
	15.9
6.02×10^{-4}	21.9
	19.9
3.28×10^{-4}	30.5
	30.7
2.11×10^{-4}	39.5
	38.1
8.33×10^{-5}	46.6
	47.3
7.65×10^{-5}	47.0
	51.0
2.36×10^{-5}	55.3
	56.4
1.16×10^{-5}	56.7
	57.1
2.75×10^{-6}	61.7
	61.2
1.35×10^{-6}	59.6
	63.6
8.10×10^{-7}	59.0
	57.0

[a]Duplicate determinations at each concentration.

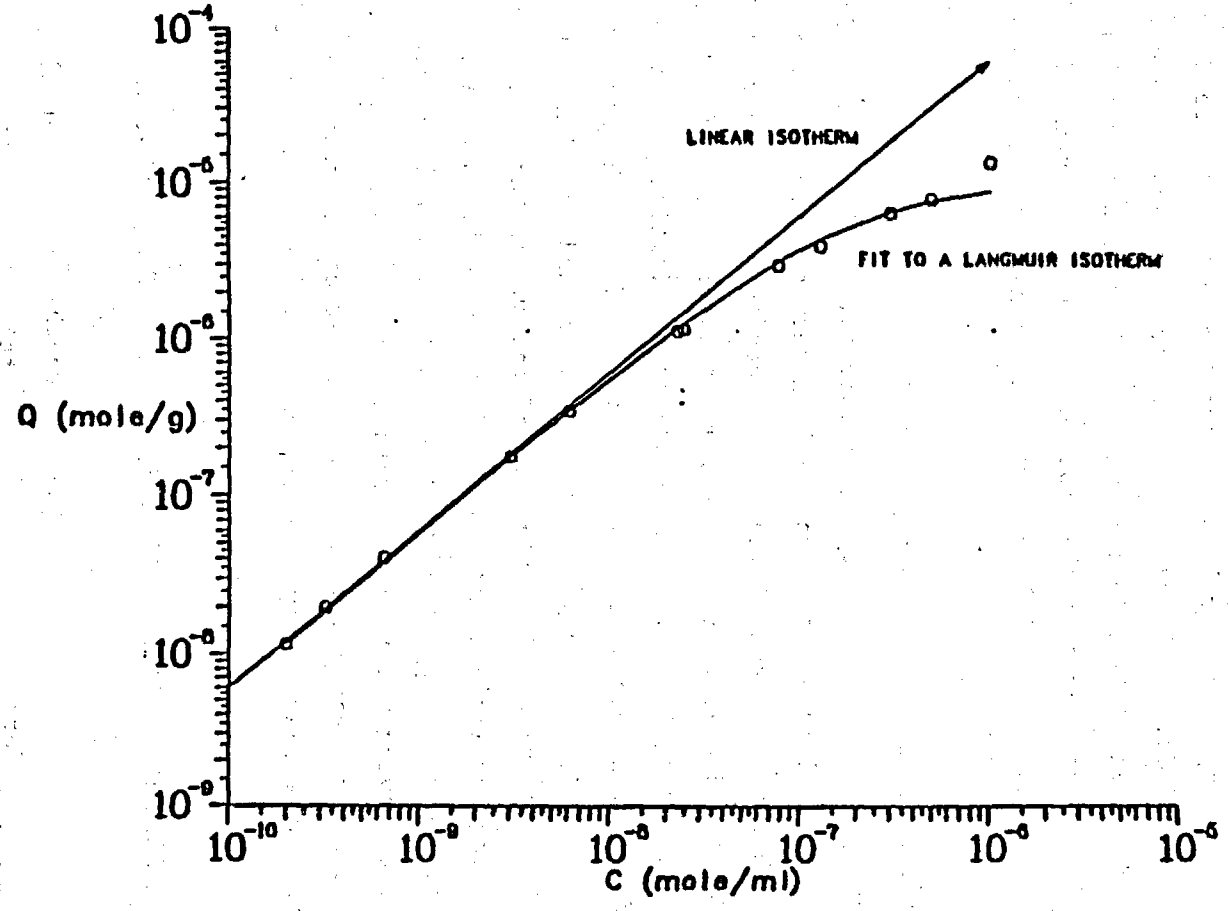

Fig. 4. Strontium sorption isotherm for G1-2840 tuff.

could be used routinely for anion determinations. Experience with the Dionex columns, using the suppressor installed on the Dionex instrument, seems to indicate that this method is much more satisfactory and straightforward.

K. Fe(II) Analyses (B. P. Bayhurst)

Analyses performed on several Yucca Mountain cores showed Fe(II) contents in the 1- to 100-ppm range or less, except for that in a core from the Tram unit in USW-G1 at 3252 ft, which was in the few per cent range (Table VIII). Trace pyrite was found at 3371 ft in this unit,[16] although none was found above this depth. Sulfide interferes in the procedure used to determine Fe(II). [The sulfide reacts with the ^{131}ICl to form $^{131}I_2$, which is the measurement for Fe(II).]

L. Natural Chemical Analogs (R. J. Vidale)

The study of geothermal sites in felsic tuffs like those of Yucca Mountain will give essential information on the long-term behavior of such tuffs in the near-field thermal gradient of the waste repository. A 3-year program plan has been developed that includes: (1) a literature search for published information on hot spring localities in Nevada and an initial selection of those that occur in felsic volcanic tuff, (2) acquisition of as much information on the localities as possible from published literature and from knowledgeable workers in the field, (3) our own investigation of the two or three most promising felsic tuff hot spring localities, and (4) a modeling effort, integrated with other transport and reaction modeling, to describe the chemical behavior of major and trace elements moving within a temperature gradient in felsic tuff.

The literature search was completed. After consideration of potential localities, a site near Beatty, Nevada, was chosen for the initial study. A

TABLE VIII

THE Fe(II) CONTENT OF CORES FROM THE YUCCA MOUNTAIN AREA

Core	Depth (ft)	Fe(II) (ppm)
Topopah UE-25a1	851	≤ 81
Bedded tuff Calico Hills USW-G2	1813	≤ 11
Bullfrog UE-25a1	2391	≤ 1
Tram USW-G1	3252	1.78×10^4

field trip was made to the Bailey Hot Springs at Beatty, and the rocks of the area were examined and sampled. The hot springs emerge from felsic tuffs like those of Yucca Mountain and over a long period of time the warm groundwater has strongly altered the felsic tuff. The samples will be analyzed for mineral phase assemblage alteration and to determine what materials have been removed by leaching by the warm groundwater and what materials have been added by precipitation from the water.

IV. MINERALOGY-PETROLOGY OF TUFF (D. L. Bish, R. E. Semarge, D. E. Broxton, F. M. Byers, B. H. Arney, G. H. Heiken, R. C. Gooley, S. Levy, and D. T. Vaniman)

A. Summary Studies

During this quarter, a summary of the mineralogy-petrology of Yucca Mountain tuffs was compiled.[17] In this summary, the findings from studies on five drill holes are related to the problems of characterizing Yucca Mountain and determining critical aspects of mineral stability. Studies of mineral stability are still in progress; studies of natural zeolite and clay compositions are also incomplete, but some of the data now available for drill core USW-G2 are summarized here.

1. Zeolites (Clinoptilolite-Heulandite). Compositional zonation in the heulandite-to-clinoptilolite series is common in the altered tuffs of Yucca Mountain, with compositions ranging from calcium- to potassium- to sodium- cation end members with increasing depth.[18] Detailed zeolite compositions have been collected in part for drill hole USW-G1 and for a more complete suite from drill hole USW-G2. The data for drill hole USW-G2 are summarized in Table IX. These data represent our current knowledge of the heulandite-clinoptilolite zonation at Yucca Mountain.

The progressive transition from heulandite to potassium-clinoptilolite to sodium-clinoptilolite is evident in Fig. 5. This is the expected pattern of variation with depth, but the details of composition (Table IX) suggest that content of the major large cations calcium, potassium, and sodium does not vary systematically with depth. For example, calcium content decreases as potassium content rises, but increases again with greater sodium content at depth. The general patterns of variation in these major large cations do not suggest any systematic depletion or enrichment with depth. The minor cations titanium and barium do not occur in concentrations significantly greater than microprobe detection limits. Content of iron is significant in some samples

TABLE IX

ZEOLITE ANALYSES FROM DRILL CORE USW-G2, YUCCA MOUNTAIN: AVERAGE COMPOSITIONS AT SIX DEPTHS[a]

	Mg-Heulandite 19 Analyses, 171-206 m Depth		Clinoptilolite 10 Analyses, 232-532 m Depth		Mg-Clinoptilolite 18 Analyses, 633-741 m Depth		Clinoptilolite 14 Analyses, 935-973 m Depth		Clinoptilolite 3 Analyses, 991 m Depth		Clinoptilolite 7 Analyses, 1064 m Depth	
SiO_2	66.0	(2.9)	66.0	(1.4)	68.3	(1.8)	68.4	(4.8)	67.1	(1.0)	69.3	(0.6)
TiO_2	0	(0)	0	(0)	0	(0)	0.05	(0.05)	0	(0)	0.02	(0.02)
Al_2O_3	13.1	(0.7)	12.4	(0.3)	12.0	(0.6)	12.0	(0.6)	11.8	(0.2)	12.5	(0.18)
FeO	0.04	(0.09)	0.04	(0.07)	0.01	(0.02)	0.33	(0.28)	0.07	(0.07)	0.03	(0.03)
BaO	0.13	(0.17)	0.06	(0.07)	0.04	(0.10)	0.07	(0.08)	0.04	(0.03)	0.01	(0.02)
MgO	1.19	(0.32)	0.08	(0.25)	0.40	(0.10)	0.01	(0.02)	0.01	(0.01)	0	(0)
CaO	4.07	(0.20)	3.27	(0.25)	3.17	(0.31)	1.50	(0.94)	2.40	(0.09)	2.12	(0.44)
Na_2O	0.18	(0.09)	1.00	(0.32)	0.69	(0.20)	3.74	(0.75)	3.65	(0.60)	2.27	(0.44)
K_2O	1.13	(0.36)	3.26	(0.44)	2.40	(0.39)	2.21	(0.74)	0.08	(0.05)	0.41	(0.14)
Σ	84.8		86.1		87.0		88.3		85.2		86.7	
Si	14.59	(0.18)	14.79	(0.11)	14.99	(0.15)	14.91	(0.26)	14.98	(0.06)	15.07	(0.07)
Ti	0	(0)	0	(0)	0	(0)	0.01	(0.01)	0	(0)	0	(0)
AL	3.46	(0.19)	3.27	(0.12)	3.10	(0.12)	3.10	(0.30)	3.09	(0.03)	3.20	(0.03)
Σ_{Tet}	18.05	(0.03)	18.06	(0.04)	18.09	(0.04)	18.01	(0.05)	18.07	(0.06)	18.27	(0.08)
Fe	0.01	(0.02)	0.01	(0.01)	0	(0)	0.06	(0.05)	0.01	(0.01)	0	(0)
Ba	0.01	(0.01)	0	(0)	0	(0)	0.01	(0.01)	0	(0)	0	(0)
Mg	0.40	(0.11)	0.01	(0.02)	0.13	(0.03)	0.01	(0.01)	0	(0)	0	(0)
Ca	0.98	(0.05)	0.78	(0.07)	0.74	(0.07)	0.36	(0.23)	0.57	(0.03)	0.50	(0.11)
Na	0.07	(0.04)	0.43	(0.14)	0.29	(0.08)	1.57	(0.24)	1.57	(0.23)	0.96	(0.19)
K	0.32	(0.10)	0.87	(0.27)	0.66	(0.11)	0.61	(0.18)	0.04	(0.04)	0.12	(0.04)
$\Sigma_{large\ cations}$	1.79	(0.08)	2.10	(0.39)	1.83	(0.20)	2.60	(0.25)	2.20	(0.19)	1.57	(0.24)
$\Sigma_{cations}$	19.84	(0.08)	20.16	(0.39)	19.92	(0.18)	20.60	(0.22)	20.27	(0.13)	19.84	(0.17)

[a]Numbers in parentheses represent one standard deviation.

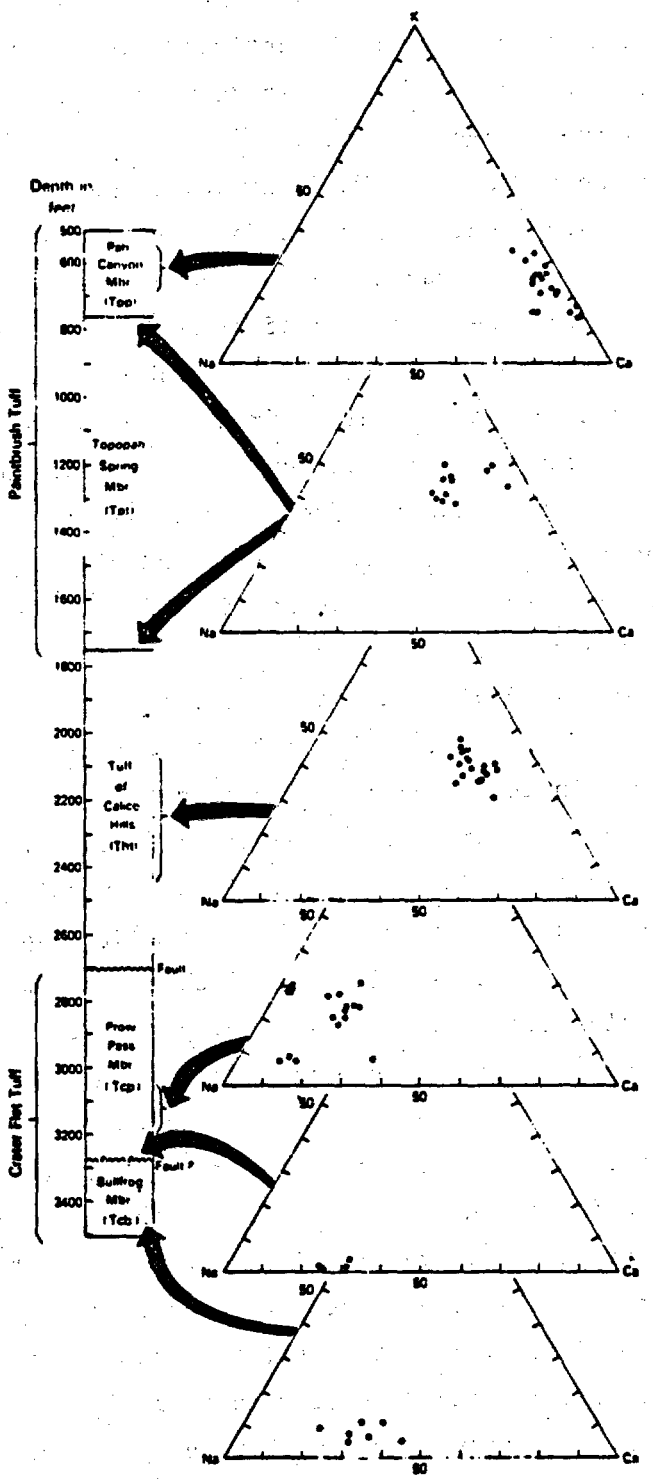

Fig. 5. Zeolite compositions in drill hole USW-G2.

at 935 to 973 m but is greatly variable between samples at this depth. Content of magnesium is significant only in the sodium-poor samples from the upper part of the core; it is not known whether the anticorrelation between sodium and magnesium is determined by depth of zeolitization or by the compositions of rock and fluid at the time of zeolitization.

Previous studies in the vicinity of Yucca Mountain suggest that large amounts of cation exchange are required for the formation of heulandite-clinoptilolite zeolites from siliceous volcanic glass. Hoover[18] suggests that the zeolite zoning took place after the formation of clinoptilolite and consisted of sodium replacement for calcium and magnesium; the high calcium and magnesium contents of the first-formed zeolites resulted from groundwater transport and concentration. Carr[19] suggests that the calcium concentration was coupled with leaching of silicon, sodium, and potassium from primary glass. The occurrence of mordenite compositions intermediate between glass and clinoptilolite-heulandite zeolites lead Carr to propose that the formation of mordenite may be a precursor to clinoptilolite-heulandite zeolitization. Many questions about the zeolite formation sequence and compositional zonation are still largely unanswered.

The thermal stability of sorptive zeolites is of potential importance to a high-level waste repository in tuff. Smyth[20] summarized the available data on zeolite stability and suggested that adverse reactions (for example, reactions that liberate water and open fractures) can be avoided by keeping the zeolite-bearing horizons saturated and at temperatures below ~85°C. Appropriate long-run experiments, however, have not been established. Such experiments are critical for determining the variable effects of temperature, water pressure, and water composition. Stability over geologic time periods can be modeled from kinetic parameters obtained from experimentation. These models will be critical to projecting stability and retardation ability into the repository's isolation period. A final but very important factor in the model will be the composition of the zeolites, which is a crucial issue in retardation. It is known that short-term heating will readily degrade heulandite at temperatures as low as 250°C, but clinoptilolite will not immediately degrade until temperatures of ~700°C are reached. This suggests that a similar disparity in thermal stability might be found at lower temperatures maintained for longer time spans (~10^2 to 10^4 years). These problems are presently under investigation.

2. Clay Minerals. Clay minerals are widespread throughout the tuffs of Yucca Mountain. Although abundances of clay are typically 5 to 15%, abun-

dances as high as 50% occur in some units. Tuffs in the upper 150 m of Yucca Mountain, which retain tridymite and cristobalite, also contain very little clay. There is, in addition, a general anticorrelation between abundances of clays and zeolites; the most zeolitized units such as the tuff of Calico Hills have the least clay. This relationship between zeolites and clays suggests that clay formation requires a permeable environment, and the decrease in permeabilty following zeolitization may inhibit clay formation. Textural evidence also suggests that clays form after zeolitizaton. Although some smectites occur as a late-stage fracture filling, most are concentrated in pumice relicts or scattered within the tuff groundmass. The smectites in the upper portions of USW-G2 are predominantly sodium- and calcium-saturated montmorillonite-beidellites (Table X) with few or no interstratified illite layers. The change from pure smectite to interstratified illite/smectite with depth is reflected both in x-ray diffraction studies and in the chemical composition of the clays (Table X). In general, the amounts of potassium and interstratified illite increase with depth, but the smectites remain expandable until ~1524 m in USW-G2. Below that depth, nonexpandable illite and chlorite are present. In USW-G2, the transition from a one-water-layer smectite to a collapsed (but still expandable) smectite takes place at ~457 m, but there are scattered occurrences of collapsed smectites above that depth and of several expanded smectites below 457 m. At depths shallower than 1067 m, randomly interstratified smectite/illites occur, with a sporadic increase in the degree of interstratification with illite with depth. Below 1067 m, there is an abrupt increase in the amount of interstratified illite, with ordered interstratifications appearing. Below 1158 m, a long-range ordered, illite-rich interstratification occurs. The material is referred to as Kalkberg-ordered (columns 5 and 7, Table X) and occurs with illite abundances between 80 and 95%.

The randomly interstratified smectite/illites occuring shallower than 1067 m are consistent with temperatures of formation of <40°C. However, the ordered illite/smectites occurring below 1067 m suggest temperatures above 100°C,[21] and the Kalkberg-ordered clays occurring below 1158 m are consistent with temperatures ranging from 180 to 230°C. Such an abrupt and, in places, sporadic increase in temperature cannot be explained simply through the imposition of a high paleogeotherm. These data, together with the occurrence of sulfides, barite, and fluorite in the lower parts of the drill holes, suggest that considerable hydrothermal alteration has taken place. There is some evidence for the presence of two generations of smectites throughout Yucca Mountain, and expandable

TABLE X

AVERAGED OR REPRESENTATIVE CLAY ANALYSES[a] FROM DRILL CORE USW-G2

	4 Analyses, Smectite in Pumice 926 m Depth		6 Analyses, Smectite in Pumice 991 m Depth		Smectite in Pumice 1065 m Depth	Smectite in Pumice 1080 m Depth	Kaikberg Clay in Pumice 1182 m Depth	Blue Smectite in Tuff Matrix 1247 m Depth	6 Analyses, Kaikberg-Type Illite-Smectite in Pumice 1362 m Depth		3 Analyses, Illite Crystal 1725 m Depth		Illite Crystal 1800 m Depth	5 Analyses Illite in Pumice 1828 m Depth	
SiO_2	55.8	(0.9)	56.2	(0.8)	55.5	51.4	47.6	56.5	53.3	(0.6)	48.5	(0.8)	52.6	52.1	(0.7)
TiO_2	0.18	(0.04)	0.18	(0.09)	0.16	0.15	0	0	0.06	(0.03)	0.70	(0.69)	0.21	0.16	(0.06)
Al_2O_3	22.9	(0.7)	20.8	(0.6)	22.2	20.4	24.8	18.1	27.1	(1.1)	27.0	(0.5)	19.4	26.6	(1.0)
FeO	2.09	(0.33)	7.1	(0.8)	5.86	6.34	3.28	1.10	2.83	(0.460)	3.17	(0.41)	9.4	4.09	(0.87)
BaO	0	(0)	0.03	(0.05)	0.03	0	0	0	0	(0)	0.17	(0.04)	0.04	0.01	(0.02)
MgO	2.68	(0.04)	1.55	(0.07)	1.61	1.91	1.30	4.11	2.40	(0.26)	2.38	(0.41)	2.64	1.82	(0.13)
CaO	2.85	(0.28)	1.48	(0.36)	1.25	0.57	0.23	1.06	0.21	(0.06)	0.03	(0.03)	0.30	0.30	(0.15)
Na_2O	0.91	(0.15)	1.31	(0.35)	0.20	0.45	0.16	0.22	0.44	(0.05)	0.05	(0.05)	0.18	0.34	(0.08)
K_2O	0.34	(0.05	1.55	(0.69)	1.99	4.95	6.42	2.34	8.39	(0.22)	9.46	(0.22)	8.82	8.65	(0.23)
Σ^b	87.9	(1.8)	90.3	(1.2)	88.9	86.3	83.8	83.4	94.8	(1.1)	91.5	(0.5)	93.6	94.0	(1.6)
Si^b	7.56	(0.04)	7.64	(0.07)	7.60	7.46	7.07	8.01	7.04	(0.05)	6.74	(0.08)	7.33	7.00	(0.13)
Ti	0.02	(0)	0.02	(0.01)	0.02	0.01	0	0	0	(0.01)	0.07	(0.07)	0.02	0.01	(0.01)
Al	0.42	(0.04)	0.34	(0.08)	0.38	0.53	0.93	0	0.96	(0.06)	1.18	(0.12)	0.65	0.99	(0.13)
Σ	8.00	8.00	8.00	8.00	8.00	8.00	8.00	8.01	8.00		8.00		8.00	8.00	
Al	3.23	(0.01)	3.00	(0.04)	3.20	2.96	3.40	3.04	3.26	(0.08)	3.25	(0.06)	2.53	3.22	(0.04)
Fe	0.24	(0.03)	0.81	(0.06)	0.67	0.77	0.40	0.12	0.31	(0.05)	0.37	(0.05)	1.10	0.45	(0.09)
Mg	0.54	(0.01)	0.31	(0.02)	0.32	0.41	0.28	0.87	0.47	(0.06)	0.49	(0.09)	0.54	0.36	(0.03)
Σ_{oct}	4.01	(0.02)	4.12	(0.04)	4.19	4.14	4.08	4.03	4.04	(0.04)	4.11	(0.08)	4.17	4.03	(0.08)
Ca	0.41	(0.04)	0.21	(0.05)	0.18	0.09	0.03	0.16	0.03	(0.01)	0	(0.01)	0.04	0.7	(0.02)
Na	0.24	(0.04)	0.35	(0.09)	0.05	0.12	0.04	0.06	0.11	(0.01)	0.01	(0.01)	0.04	0.09	(0.02)
K	0.06	(0.01)	0.27	(0.12)	0.35	0.92	1.21	0.42	1.41	(0.03)	1.68	(0.04)	1.56	1.48	(0.03)
Ba	0	(0)	0	(0)	0	0	0	0	0	(0)	0.01	(0.01)	0	0	(0)
$\Sigma_{interlayer}$	0.70	(0.02)	0.82	(0.04)	0.58	1.13	1.28	0.64	1.55	(0.04)	1.70	(0.03)	1.64	1.61	(0.03)

[a] Numbers in parentheses represent one standard deviation.

[b] Under the high-vacuum and heating effects of electron microprobe analysis, the weight percent total analyses of most clays should total between 90 and 95%. Many of the clays listed have lower totals that reflect the analysis of fine-grained minerals in an epoxy-impregnated thin section: The low totals may result from the admixture of epoxy with clay, but the analyses are reported if the formula stoichiometry is correct. Stoichiometric calculations are based on a 20-oxygen, 4-OH (or 22 oxygen equivalent) formula. On this basis, the tetrahedral site occupancy is assumed to be eight, with dioctahedral site occupancy ≈4.00 and a total between 0.7 and 1.7 for interlayer cation content. Special note should be made of those samples with exceptionally high octahedral site occupancy (>4.00) and/or low interlayer cation content (<0.67); in these samples stoichiometry might be maintained by recalculating some of the Mg as an interlayer rather than as an octahedrally coordinated cation (Mg can occur as an exchangeable cation in many smectite clays).

smectites coexist with collapsed smectites in scattered samples down to about 1524 m in USW-G2. For example, the presence of a smectite with little or no interstratified illite at 1508 m in USW-G2, determined by x-ray diffraction, demonstrates that low-temperature alteration has taken place after the higher temperature hydrothermal alteration. This type of occurrence is evidence that hydrothermal alteration has not been pervasive for some time. Although hydrothermal alteration may be considered to be an unlikely future event, it might be advisable to date mineralized veins to determine the age of this hydrothermal system.

The stabilities of sodium- and calcium-smectites over geologic time spans are still poorly constrained. The effects of illite interstratification on smectite sorptive capabilities directly relate to the percentage of illite allowable if high cation exchange capacities are to be retained. As with zeolites, the properties of smectites that are favorable for the high-level-waste repository isolation period are dependent on temperature, water pressure, and water composition. Experiments now in progress will take these variables into consideration.

B. Re-examination of Reported Erionite and Phillipsite Occurrences at Yucca Mountain

During this quarter, some reported occurrences of the zeolites erionite and phillipsite in drill hole J-13, and of erionite in drill hole UE25a-1h were reinvestigated. The reinvestigation, based on the same samples, showed no erionite or phillipsite in amounts above current detection limits by x-ray diffraction (~3%) in either drill hole. The previous descriptions were made either without the benefit of x-ray diffraction analysis or by much less precise x-ray diffraction methods than those currently in use (Appendixes).

C. Ongoing Drill Core Studies

Studies are in progress on drill cores USW-G3 and USW-GU3 and on bit cuttings and sidewall samples from hydrology holes USW-H3, USW-H4, and USW-H5. X-ray diffraction analysis for USW-G3/USW-GU3 confirms the petrologic observation that this drill hole is predominantly vitric from 1195 ft to 1598 ft depth, with the first appearance of clinoptilolite as a major phase at 1827 ft depth. Analcime first appears in significant amounts at 3936 ft and is present to the bottom of the hole.

Petrographic studies of thin sections from 11 sidewall samples and bit cuttings from USW-H4 indicate that parts of the upper section (1312 ft depth) contain ~20 to 25% glass rimmed by cristobalite. However, the underlying samples are heavily zeolitized (1420 to 1550 ft depth) or otherwise devitrified. Prepared specimens from hydrology holes USW-H3, USW-H4, and USW-H5 are now ready for electron microbeam and x-ray diffraction studies.

V. VOLCANISM STUDIES (W. S. Baldridge, F. Caporuscio, B. M. Crowe, and D. T. Vaniman)

A paper by Vaniman et al.,[23] submitted to "Contributions to Mineralogy and Petrology," summarizes the current status of volcanism studies at Crater Flat, Nevada. Hawaiite-type lavas were erupted in three cycles (3.7, 1.2, and 0.3 Myr) at Crater Flat. The compositions of all three cycles, considered together, form a "straddling" alkalic series as defined by Miyashiro,[24] in which the less evolved basalts plot near the normative olivine-diopside divide and the more evolved basalts project into the hypersthene or nepheline fields. Fractionation modeling based on the oldest cycle allows the removal of olivine, clinopyroxene, and amphibole to arrive at the more evolved hawaiite compositions. In general, fractionation of phlogopite or feldspar is limited by the fractionation modeling and by europium/rare-earth element relations. In detail, all hawaiites within one cycle (3.7 Myr) cannot be derived from a single parent magma. Varied parentage is evident between cycles as well, although all cycles are consistently of hawaiite composition. Basalts of the youngest two cycles are generally enriched in trace elements. Superimposed on this enrichment is a lack of rubidium variation, leading to rubidium/strontium ratios far lower than those required to generate the high $^{87}Sr/^{86}Sr$ ratio (0.707) typical of basalts in this region. The very low rubidium/strontium ratios limit processes that may lead to trace-element enrichment during magma evolution (cyclic recharge of a fractionating magma chamber). Decreased fractions of mantle melting, leaving phlogopite in the residuum, or an earlier event of metasomatic transport from phlogopite-bearing mantle rocks into a phlogopite-absent mantle assemblage might explain the observed trace-element enrichment with low rubidium/strontium.

A paper by Crowe et al.,[25] submitted to "Journal of Geology," discusses the aspects of possible magmatic disruption of a high-level waste repository in southern Nevada. The NTS region is located in the central section of a N-NE trending basaltic volcanic belt of late Cenozoic age, a part of the Quaternary

volcanic province of the Great Basin. Future volcanism within the belt represents a potential hazard to storage of high-level radioactive waste within a buried repository located in southern Nevada. The hazards of future volcanism in the region are being characterized through a combination of volcanic hazards studies, probability determinations, and consequence analyses. Basaltic activity within the NTS region is divided into two age groups consisting of relatively large-volume silicic cycle basalts (8 to 10 Myr) and rift basalts (<8 to 0.3 Myr). The rift basalts occur as small-volume (<0.1-km^3), spatially separate basaltic centers. The lavas are classified as hawaiites and show strong affinities to the alkalic basalt suite. They were derived from the upper mantle below a depth of 30 to 35 km and were modified from parental compositions by crystal fractionation. Younger rift basalts (<4 Myr) are enriched in incompatible trace elements. Theoretical and geological considerations of basalt rise rates indicate rapid ascent of basalt (tens of cm/second) within the bubble-free regime. Rising basalt magma is probably trapped at the crust/mantle density interface. The magma probably crystallizes high-density phases (olivine, pyroxene) that decrease the liquid density due to crystal removal. As the density decreases, the magma reinitiates rapid ascent through the crust. Field studies and geometrical arguments suggest that basalt centers are fed at depth by narrow, linear dikes (aspect ratio 10^{-2} to 10^{-3}). However, in some cases, shallow instrusions are formed (Paiute Ridge and Nye Canyon area of the NTS). These intrusions probably formed through a combination of factors during emplacement, including extension faulting and trapping by low-density tuff as a result of low volatile content in the magma. Surface basalts comprise single or coalesced scoria cones of moderate size with associated lava flows. Eruptions were predominantly of Strombolian type. The rise rate of basalt magma for these centers was probably toward the low range of typical basalt rise rates, based on their ratios of cone volume to lava volume and their short lava flow lengths. It is assumed that waste elements are incorporated and transported in basalt magma in a manner similar to that of lithic fragments. Such fragments are probably engulfed during magma disruption and fragmentation and are partitioned preferentially in the pyroclastic component of an eruption. Assuming a future magmatic cycle of volume similar to that of the Lathrop Wells cone of the NTS region, 54 m^3 of material from a repository horizon will be deposited in a scoria cone (of which 2.7 m^3 will be exposed at the surface in a 10 000-year period), 96 to 245 m^3 will be incorporated in a scoria sheet (2 to 12 km dis-

persal) and 6.1 m^3 will be dispersed regionally with the fine-grained particle fraction (>12 km dispersal).

VI. ROCK PHYSICS STUDIES (J. D. Blacic)

This quarter the first creep test at elevated temperature and pressure was performed. Although the test was not completely successful because of a jacket leak, some interesting results were obtained.

The test specimen was a tuff from the Bullfrog Member at the 2483-ft level of hole drill USW-G1. The sample was 11.1 cm long and 5.4 cm in diam. The test conditions were 100°C, 50 MPa differential stress, 20 MPa confining pressure, and 5 MPa water pore pressure. The effective confining pressure of 15 MPa was attained initially, but as a result of a slow jacket leak that developed early in the test, the effective pressure slowly dropped over the duration of the test to ~50% of the initial value. Because of the slow decrease in effective pressure, axial strain actually decreased slowly from the initial loading value while circumferential strain increased slowly. Over the last 20 hours of the test the average circumferential strain rate was ~1.2×10^{-9}/second, which increased very slightly in the last 2 hours. In retrospect, this almost imperceptible increase in strain rate reflected the onset of a type of tertiary creep that only developed strongly in the last 200 seconds of the test. Strain accelerated rapidly during this period, and the sample failed at a total test time of ~69 hours.

This type of sudden tertiary creep failure is similar to that observed in uniaxial, room temperature creep of Grouse Canyon welded tuff. In each case there has been little indication of the nearness to failure and, so far, no evidence of the classical exponentially increasing tertiary creep that has been observed in granite and other materials. This may be a reflection of the textured inhomogeneity of welded tuff samples. Failure may initiate in a very local region with no general increase in microfracturing activity that might be noticeable at strain gauges outside of the ultimate failure zone.

Although this test alone does not establish a new issue of concern, it does suggest a type of potential failure that should be evaluated. In the near field of a repository in a material of very low permeability and relatively high water content, such as a zeolitized tuff, thermal expansion of pore water or mineral dehydration water could lead to a local increase in pore pressure if the water could not leak off rapidly enough. The increase could lead to

local rock failure initiation because of the reduction in effective pressure. This would occur while at least some of the strain monitors were indicating a decreasing rate of strain caused by the decompression associated with a falling effective pressure.

VII. SHAFT AND BOREHOLE SEALING (R. J. Vidale)

The purpose of this study is to evaluate the short- and long-term chemical stability of sealing materials in the felsic tuff environment of Yucca Mountain. A 3-year program plan has been developed. Initial tests for the purpose of screening a number of potential sealing materials include agitated-vessel studies to accelerate reaction at 25 to 200°C. Samples will be examined before and after tests by x-ray diffractometer, optical microscope, scanning electron microscope, and electron microprobe. The most promising candidates for sealing materials will also be tested in a temperature gradient circulating system. Rock and cement permeability tests may also be run at controlled temperature and pressure. Field tests of selected materials will consist of flow tests in which a fluid pressure differential is imposed on a sealed borehole. Such tests will include observation of chemical reaction in the disturbed region adjacent to the borehole in addition to that in the sealed hole. The hole will later be overcored and dissected; the rock and sealing material will be examined in detail for chemical interaction by the methods described above.

Two samples of G-Tunnel tuff were obtained from Sandia National Laboratories so that geochemical testing can be initiated on the same material that the Waterways Experiment Station is using to determine mechanical properties for Sandia.

A visit was made to the Materials Research Laboratory at Pennsylvania State University to discuss the sealing studies being done at that laboratory and explore the feasibility of further work during FY 1983. The geochemical part of such work would include the studies of the chemical interaction of felsic tuff with sealing materials in agitated vessels and in circulating systems, followed by detailed examination of the experimental samples to determine the nature of sealant/rock interaction.

VIII. EXPLORATORY SHAFT (D. C. Nelson, S. D. Francis, T. J. Merson, and W. L. Sibbitt)

It appears that the DOE will authorize accelerating activities in the NNWSI project to allow drilling of the Exploratory Shaft (ES) 6 months earlier than previously planned. Some of the major milestones are shown below.

	Accelerated Schedule	Planned Schedule
Spud principal borehole	7/82	not established
Start shaft drilling	3/83	9/83
Complete mining and start horizontal borings	4/84	2/85
Submit site recommendation report	4/85	?/87

The accelerated schedule is based upon the assumptions that the Test and Evaluation Facility will not be constructed at the NNWSI site and that the unsaturated horizons will be investigated first with the capability to extend the ES to the saturated horizons, should the unsaturated zone be found unacceptable.

The ES activities are proceeding on the basis that shaft construction will start in March 1983, although an official decision has not been made. Four key decisions that must be made before detailed design of the ES can proceed very far are (1) ES construction method, (2) ES location, (3) ES depth, and (4) number of breakouts. An ad hoc working group was established in April 1982 to identify a mechanism for making a recommendation on the first two decision issues. This group was charged with the responsibility for implementing the decision-making process and submitting its recommendations to the Technical Overview Officer (TOO). The findings of the committee concerning the construction method have been forwarded to the TOO recommending that the shaft be conventionally sunk. The committee determined that several sites can meet scientific and constructibility criteria and recommended a site located at ~4150 ft elevation in the wash containing test hole UE25a-6.

The ES design and procurement activities will be initiated by Los Alamos by transmitting design criteria letters (DCL) to DOE/NTSSO, who will, in turn, approve and transmit them to the appropriate NTS support contractor. Two DCLs have been prepared and issued. The first authorizes preparation of specifications for breaking tongs, communication shelters, a mine cage communication system, and electrical transformers. The FY 1982 capital equipment funds are

available for these items. The second DCL authorizes preparation of specifications for the main hoisting system.

A draft Program Management Plan was submitted to DOE/NV for review. A schedule and work plan have not been fully developed. These will be developed in conjunction with Fenix and Scisson and Holmes and Narver after both the shaft construction method and location have been selected.

IX. QUALITY ASSURANCE (P. L. Bussolini, R. R. Geoffrion, A. H. Davis, H. Nagel, and F. L. Kerstiens)

A. Los Alamos National Laboratory

Several meetings were held with technical personnel to gather information for a Technical Review of Publications procedure. A draft of the procedure has been prepared and distributed for comment.

The QA office reviewed a Notebook for Quality Assurance for NNWSI work; comments were presented at a QA-Interface Coordination Group meeting.

QA personnel transmitted their comments on the ES Conceptual Design Report to Los Alamos NNWSI office and NNWSI, and potential repository sites were examined at the NTS. The QA section for the ES Project Management Plan was prepared and given to the Los Alamos NNWSI office.

Procedures and work plans are being revised to be consistent with Los Alamos report format. Some of the procedures recently revised are the QA Program Plan, the Document Control procedure, the Volcanic Hazards Work Plan, the Work Plan for Actinide Chemistry, the Mineralogic and Petrologic Studies Work Plan, and the Siemens X-Ray Diffraction procedure.

An internal audit was performed for procurement activities of the Los Alamos NNWSI work on May 12.

Answers to the DOE-NV/Overview audit 82-3 were written and distributed.

B. US Geological Survey

An audit was conducted by DOE in Denver and at the NTS. Los Alamos QA personnel represented the USGS at all QA audit meetings. Answers prepared in response to the DOE/NV audit findings were sent to the USGS.

Revisions to the Gravity Measurements and Data Reduction Procedure, the Earthquake Location Procedure, and the Methods for Determination of Radioactive Substances in Water Procedure were distributed to holders of the USGS Manual of QA Procedures. A draft of the QA Peer Review Procedure has been prepared. The

Instrument Calibration Procedure for Seismic Studies has been established and sent out for approvals. The QA office reviewed and commented on a Notebook for Quality Assurance for NNWSI work. Comments were presented at a QA-Interface Coordination Group meeting.

A meeting was held with Fenix and Scisson personnel to develop a plan for their participation in the USGS drilling program.

At the Nuclear Regulatory Commission technical sessions held in Las Vegas and at NTS, QA personnel made a presentation on the USGS Program.

ACKNOWLEDGMENTS

The following Los Alamos National Laboratory personnel are acknowledged for their efforts: D. A. Mann (technical assistance); P. A. Elder, M. E. Lark, and S. Lermuseaux (sample counting and gamma-spectral analyses); and C. E. Gallegos (typing of drafts and final manuscript).

REFERENCES

1. K. Wolfsberg, W. R. Daniels, D. T. Vaniman, and B. R. Erdal, Comps., "Research and Development Related to the Nevada Nuclear Waste Storage Investigations, October 1 - December 31, 1981," Los Alamos National Laboratory report LA-9225-MS (April 1982).

2. I. J. Winograd and F. N. Robertson, "Deep Oxygenated Ground Water: Anomaly or Common Occurrence?" Science 216, 1227-1230 (1982).

3. A. I. Moskvin and A. D. Gel'man, "Determination of the Composition and Instability Constants of Oxalate and Carbonate Complexes of Plutonium(IV)," J. Inorg. Chem., USSR 3 198-216 (1958).

4. R. J. Lemire and P. R. Tremaine, "Uranium and Plutonium Equilibria in Aqueous Solutions to 200°C," J. Chem. Eng. Data 25, 361-369 (1980).

5. T. J. Wolery, "Calculation of Chemical Equilibrium Between Aqueous Solution and Minerals: The EQ3/6 Software Package," Lawrence Livermore Laboratory report UCRL-52658 (February 1979).

6. W. R. Daniels et al., "Summary Report on the Geochemistry of Yucca Mountain and Environs," Los Alamos National Laboratory report LA-9328-MS (in preparation, 1982).

7. J. M. Cleveland, The Chemistry of Plutonium (American Nuclear Society, La Grange Park, Illinois, 1979), pp. 105-127.

8. J. F. Kerrisk, "Chemical Equilibrium Calculations for Aqueous Geothermal Brines," Los Alamos National Laboratory report LA-8851-MS (May 1981).

9. D. Langmuir, "Techniques of Estimating Thermodynamic Properties for Some Aqueous Complexes of Geothermal Interest," in Chemical Modeling in Aqueous Systems, E. A. Jenne, Ed. (American Chemical Society, Washington, D.C., 1979), Chap. 18, pp. 353-387.

10. I. Grenthe, D. Ferri, and F. Salvatore, "Actinide Carbonate Complexes and Their Importance for Radionuclide Migration," Department of Inorganic Chemistry, Royal Institute of Technology, Stockholm, Sweden, report TRITKA-OOK-2019 (October 1980).

11. W. R. Daniels, K. Wolfsberg, D. T. Vaniman, and B. R. Erdal, Eds., "Research and Development Related to the Nevada Nuclear Waste Storage Investigations, July 1 - September 30, 1981," Los Alamos National Laboratory report LA-9095-PR (January 1982).

12. D. Rai and J. L. Swanson, "Properties of Plutonium(IV) Polymer of Environmental Importance," Nucl. Technol. 54, No. 1 (1981).

13. L. M. Toth and H. A. Friedman, "The IR Spectrum of Pu(IV) Polymer," J. Inorg. Nucl. Chem. 40, 807 (1978).

14. E. N. Treher and N. A. Raybold, "The Elution of Radionuclides Through Columns of Crushed Rock from the Nevada Test Site," Los Alamos National Laboratory report LA-9329-MS (August 1982).

15. W. R. Daniels, B. R. Erdal, D. T. Vaniman, and K. Wolfsberg, Comps., "Research and Development Related to the Nevada Nuclear Waste Storage Investigations, January 1 - March 31, 1982," Los Alamos National Laboratory report LA-9327-PR (August 1982).

16. R. S. Spengler, F. M. Byers, Jr., and J. B. Warner, "Stratigraphy and Structure of Volcanic Rocks in Drill Hole USW-G1, Yucca Mountain, Nye County, Nevada," US Geological Survey open file report 81-1349 (1981).

17. D. L. Bish, D. T. Vaniman, F. M. Byers, Jr., and D. E. Broxton, "Summary of the Mineralogy-Petrology of Tuffs of Yucca Mountain and the Thermal Stability of Secondary Phases in Tuffs," Los Alamos National Laboratory report LA-9321-MS (in preparation, 1982).

18. D. L. Hoover, "Genesis of Zeolites, Nevada Test Site," in "Nevada Test Site," Geol. Soc. Am. Mem. 110, 275-284 (1968).

19. W. J. Carr, "Geology and Test Potential of Timber Mountain Caldera Area, Nevada," USGS Technical Letter NTS-174 (1966), pp. 25-29.

20. J. R. Smyth, "Zeolite Stability Constraints on Radioactive Waste Isolation in Zeolite-Bearing Volcanic Rocks," J. Geology 90, 195-201 (1982).

21. E. A. Perry, Jr. and J. Hower, "Burial Diagenesis on Gulf Coast Pelitic Sediments," Clays and Clay Mineral. 18, 165-177 (1970).

22. B. M. Crowe, D. T. Vaniman, and W. Carr, "Status of Volcanic Hazards Studies for the Nevada Nuclear Waste Storage Investigations," Los Alamos National Laboratory report LA-9325-MS (in preparation, 1982).

23. D. T. Vaniman, B. M. Crowe, and E. S. Gladney, "Petrology and Geochemistry of Hawaiite Lavas from Crater Flat, Nevada," submitted to Contrib. Mineral. Petrol. (1982).

24. A. Miyashiro, "Nature of Alkalic Volcanic Rock Series," Contrib. Mineral. Petrol. 66, 91-104 (1978).

25. B. M. Crowe, R. Amos, F. V. Perry, S. Self, and D. T. Vaniman, "Aspects of Possible Magmatic Disruption of a High-Level Radioactive Waste Repository in Southern Nevada," Los Alamos National Laboratory report LA-9326-MS (in preparation, 1982).

APPENDIX A

RE-EXAMINATION OF JA AND YM SAMPLES POSSIBLY CONTAINING ERIONITE AND PHILLIPSITE

Los Alamos
Los Alamos National Laboratory
Los Alamos, New Mexico 87545

memorandum

TO B. Erdal, CNC-7, MS 514

DATE June 24, 1982

FROM D. Bish Dave Bish

MAIL STOP/TELEPHONE J978/7-4337

SYMBOL ESS-2

TWS-ESS-2-6/82-14
page 1 of 2

SUBJECT RE-EXAMINATION OF JA AND YM SAMPLES POSSIBLY CONTAINING ERIONITE AND PHILLIPSITE

As you know, there is mention of erionite and phillipsite in Los Alamos reports. Heiken and Bevier (1979, LA-7563-MS) reported erionite in JA-15, JA-32, and JA-33BC, and phillipsite in JA-13. These analyses were based primarily on electron microprobe data, although the discussion of JA-32 included the x-ray diffraction (XRD) identification of "Er'ionite'(?)." Sykes, Heiken, and Smyth (1979, LA-8139-MS) reported the occurrence of erionite in YM-34 based on scanning electron microscope (SEM) examination.

I have re-examined all of the above samples by x-ray diffraction and find no evidence for the occurrence of either erionite or phillipsite. The results of my analyses are included, and they agree with previously published analyses of JA-32 (reported in memo from M. Sykes to B. Erdal, Aug. 6, 1981, #CNC7-81-180) and YM-34 (published in Carroll, Caporuscio, and Bish, 1981, LA-9000-MS). The minimum detection limits for phases such as erionite, phillipsite, mordenite, and clinoptilolite are on the order of 1-3%. In addition, the x-ray patterns of these zeolites are distinctive and their identification by XRD is usually unambiguous.

There are several explanations for the previous erionite and phillipsite identifications. All of the JA erionite and phillipsite analyses relied upon microprobe data. It is difficult, if not impossible, to obtain reliable chemical data for hydrous, finely intergrown materials, and identifications based upon analyses of such materials are suspect. Furthermore, it is possible for several different zeolites to yield similar chemical analyses, particularly erionite and mordenite.

The tentative identification of erionite in YM-34 was based on the morphology observed with the SEM. However, we have since observed identical morphologies in mordenite-rich tuffs containing no phillipsite. I suggest that the fibrous material in YM-34 is mordenite even though no mordenite peaks appeared in the x-ray diffraction pattern; we have often seen mordenite in tuffs (Topopah Spring, soak test samples) using the SEM when no mordenite peaks appeared in the x-ray diffraction patterns.

cc: B. Crowe, CNC7, MS 514
W. Myers, ESS-1, MS D461
W. Morris, ESS-2, MS K586
TWS file, MS K586

X-RAY ANALYSES OF JA AND YM SAMPLES

JA-13

Smectite	1-3%
Mica	1-3%
Quartz	10-20%
Alkali Feldspar	70-90%

JA-15

Mica	1-3%
Quartz	30-40%
Alkali Feldspar	60-70%

JA-32

Smectite	1-3%
Mica	2-5%
Quartz	30-40%
Alkali Feldspar	55-65%

JA-33

Smectite	2-4%
Mica	3-5%
Quartz	30-45%
Alkali Feldspar	50-60%

YM-34

Smectite	~5%
Clinoptilolite	60-80%
Mordenite	5-10%
Quartz	5-15%
Alkali Feldspar	5-10%

REFERENCES

1. G. H. Heiken and M. L. Bevier, "Petrology of Tuff Units from the J-13 Drill Site, Jackass Flats, Nevada," Los Alamos Scientific Laboratory report LA-7563-MS (February 1979).

2. M. L. Sykes, G. H. Heiken, and J. R. Smyth, "Mineralogy and Petrology of Tuff Units from UE25a-1 Drill Site, Yucca Mountain, Nevada," Los Alamos Scientific Laboratory report LA-8139-MS (November 1979).

3. P. I. Carroll, F. A. Caposuscio, and D. L. Bish, "Further Description of the Topapah Spring Member of the Paintbrush Tuff in Drill Holes UE25a-1 and USW-G1 and the Lithic Rich Tuff in USW-G1, Yucca Mountain, Nevada," Los Alamos National Laboratory report LA-9000-MS (November 1981).

APPENDIX B

X-RAY DIFFRACTION DATA FOR YUCCA MOUNTAIN TUFF SAMPLES

LOS ALAMOS NATIONAL LABORATORY
UNIVERSITY OF CALIFORNIA
LOS ALAMOS, NEW MEXICO 87545
Telephone Ext:

OFFICE MEMORANDUM

TO B. R. Erdal, CNC-7 DATE: August 6, 1981

FROM : M. L. Sykes, CNC-7

SUBJECT : X-RAY DIFFRACTION DATA FOR YUCCA MOUNTAIN TUFF SAMPLES

SYMBOL : CNC7-81-180

MAIL STOP : 514

The following table summarizes the best of the presently available x-ray diffraction (XRD) data for Yucca Mt. tuff samples being used in sorption experiments. Where large discrepancies existed between different analysts' results, the samples were checked under the microscope.

Systematic differences still exist between different sample sets. The greatest problem is in determination of cristobalite (SiO_2) and alkali feldspar ($(Na,K)AlSi_3O_8$) content; the major peaks of these two phases overlap. Each analyst has his own interpretation of these data (eg. Bish assumes feldspar and little/no cristobalite, Smyth and Copp assume about equal amounts of each). It is very difficult to resolve this problem petrographically due to the fine grained nature of most samples.

Also given are density and welding charactertics, oxidation state of opaque minerals, and percentage crystals and lithics. Density/welding can give a rough estimate of porosity, while percentage lithics is a measure of sample inhomogeneity.

MS:cg

cc: D. Bish, G-9, MS-978
W. R. Daniels, CNC-11
R. S. Rundberg, CNC-11
E. N. Treher, CNC-7
K. Wolfsberg, CNC-7
CNC-7 File

Table: X-ray diffraction data, Yucca Mountain tuffs. ND, not determined; NA, not applicable.

a. Dry bulk density in gm cm^{-3}. Welding refers to degree of sample compaction. N, non welded; P, partly welded; M, moderately welded; D, densely welded; V, very densely welded (vitrophyre); W, indeterminate degree of welding. UE25a-1 data from ref. 11; USW-G1 data from ref. 5, J-13 from ref. 7.

b. See ref. 4 for explanation; data from ref. 4 and F. Caporuscio, personal communication.

c. Percent crystals and lithics from petrographic modes. J-13 data from ref. 7; UE25a-1 data from ref. 11; USW-G1 data from F. Caporuscio, personal communication.

d. Percentages determined by x-ray diffraction analysis; glass determined separately. Data shown for each sample are from first reference listed; additional references give additional, contradictory or incorrect data. Abbreviations: MNT, montmorillonite; ILL/MIC, illite/mica; CPT, clinoptilolite; CR, cristobalite; q, quartz; SAN, sanidine; PLAG, plagioclase.

* Conflicting analyses, unresolved.

Unit	Sample (depth, m)	Density/ Welding[a]	Oxidation State[b]	Percent Crystals[c]	Percent Lithics[c]	Percent Glass	Percent Clay & Mica[d]	Percent Zeolite[d]	Percent SiO_2[d]	Percent Feldspar[d]	Reference[d]
DRILL SITE J-13											
Tiva Canyon	JA-6(185)	MD/M	ND	8.9	6.7	25-50	25-50 MNT	0	10-20 CR	tr	9
Topopah Springs	JA-18(433)	MD/M	C3(2-5)	1.8	11.9	~50	~5 MNT ~5ILL/MIC	5-10 CPT	15-25 CR	15-25	2,8,13,10
Prow Pass (base)	JA-26(606)	MD/M	ND	18.3	1.0	0	0	tr cpt 30-50 ALC	30-50 Q tr CR	10-20	9
Bullfrog	JA-28( )	MD/M	ND	(20)	(5)	0	tr MNT 2-5ILL/MIC	30-50 ALC	40-60 Q	10-20	9
Bullfrog	JA-32(772)	MD/W	C6(5-7)	12.6	0	0	5-10ILL/MIC	0	40-50 Q	30-40	8,10
Lithic rich tuff	JA-37(1066)	MD/M	C6(5-7)	12.6	11.0	0	20-40 MNT 5ILL/MIC	~5 CPT	30-60 Q	15-30	2,8,10
DRILL SITE UE25A-1											
Tiva Canyon	YM-5 (76.5)	MD/M	ND	10.9	4.3	~70	~10 MNT	0	<5 Q <5 CR	5-10 SAN 5-10 PLAG	9,13
Topopah Springs	YM-22(258.5)	2.3/D	C6(2-7)	1.0	0.4	0	5-10 MNT	0	40-60 Q	40-60	3,10
Topopah Springs	YM-30(385.4)	2.1/D	C5(2-7)	2.1	21.6	0	5-10 MNT ~5 MIC	5-10 CPT	40-60 Q 5-15 CR	30-50	3,9
Calico Hills	YM-38(458.7)	1.8/M	C5(4-6)	4.0	7.7	0	2-5 MNT	40-60 CPT	5-10 Q 15-30 CR	20-30	10
Calico Hills (base)	YM-42(556.1)	2.3/MA	ND	15.6	46.6	0	<5 MIC/ILL	20CPT(HEUL)	35-40 Q	~20 SAN ~20 PLAG	9,13
Prow Pass	YM-45(588.4)	MD/M	C4(3-5)	13.5	8.6	0	2-5 MNT	0	40-60 Q tr CR	30-50	10
Prow Pass	YM-46(610.1)	2.2/D	ND	12.7	0.3	0	<5ILL/MIC	0	40-60 Q	~25 SAN 20-25 PLAG	1, 9
Prow Pass	YM-48(644.2)	2.0/P	C6(5-7)	8.0	1.4	40-60	tr MNT	10-20 CPT	0	20-30	10
Prow Pass	YM-49(676.8)	1.9/M	C5(4-6)	7.6	3.4	0	0	~60 CPT	~10 Q ~10 CR	~15	13,10
Bullfrog	YM-54(759.3)	2.1/W	C5(4-7)	17.8	0.0	0	tr MNT tr MIC/ILL	0	~60 Q	~30	13,10

Unit	Sample (depth, m)	Density/ Welding[a]	Oxidation State[b]	Percent Crystals[c]	Percent Lithics[c]	Percent Glass	Percent Clay & Mica[d]	Percent Zeolite[d]	Percent SiO_2[d]	Percent Feldspar[d]	Reference[d]
DRILL SITE USW-G1											
Topopah Springs	G1-1292	MD/W	C1	MD	MD	80-90	tr MNT	0	5-10 CR	10-20	4,1
Calico Hills	G1-1436	1.6/M	C6(5-7)	5.2	3.2	0	<5 MNT <5 ILL/MIC	75-95 CPT	5-10 Q	~5	1,4
Prow Pass	G1-1883	1.7/P	C4(3-5)	16.6	1.0	0	<10 MNT <5 MIC	0	30-50 Q	50-70	1,4
Prow Pass	G1-1982[e]	1.8/M	C2	13.2	0.4	0	5-10 MNT tr MNT	0	5-15 Q 40-60 CR	70-90 30-50	1 4
Upper Bullfrog	G1-2233	1.5/M	C6(6-7)	15.4	0.4	0	<5 MNT 10-15 MIC	15-30 CPT <5 MRD	5-10 Q <5-10 CR	40-60	1,PC,4
Upper Bullfrog	G1-2289	1.6/M	C6(5-7)	15.8	1.0	0	5-10 MCI	30-50 CPT 10-20 MRB	<5 Q	30-50	1,4
Upper Bullfrog	G1-2363	1.9/M	C6(5-7)	20.4	0.2	0	10-20 MNT 5-10 MIC	0	30-50 Q	30-50	1,4
Upper Tram	G1-2698	1.8/M	C6(5-7)	13.2	1.0	0	<5 MNT 10-15 MIC	30-50 CPT <5 MRD	<5 Q	30-50	1,4
Upper Tram	G1-2901	MD/W	C6(6-7)	16.5	2.0	0	5-10 MNT 5-10 MIC	0	20-40 Q	40-60	1,4
Tram	G1-3116	1.9/MD	C6(6-7)	4.0	21.4	0	5-10 MNT 5-10 MIC	5-15 CPT 10-30 ALC	20-40 Q	20-40 Q	1,4
Flow Breccia	G1-3658	2.3/MA	C3	23.4	0.0	0	40-60 MNT	0	0	40-60	1,4

References

1. Bish, D., 1981 (Feb. 18) Memo to L. Vine, X-ray Diffraction Analyses of Pre-chemistry G-1 Core Samples.
2. Bish, D., 1981 (May 6) Memo t A. Mitchell: X-ray Diffraction Analyses of the JA-18 and JA-37 Tuff Samples (Pre-chemistry).
3. Bish, D., 1981 (June 30) Memo to distribution: X-ray Diffraction Results for UE25a-1 Topopah Springs Tuff.
4. Carroll, P. R. and A. C. Waters (editors) Preliminary Stratigraphy and Petrologic Characterization of Core Samples from USW-G1, Yucca Mountain, Nevada. LA-8840-MS.
5. Copp, J., F. Caporuscio and J. Purson, 1980 (?) Memo to?: X-ray Diffraction Analyses of USW-G1 Tuff Samples with Some Density Measurements.
6. DeVilliers, S. J., et al. 1981, Status Repor: Sorptive Properties of Yucca Mountain Tuff from Drill Hole USW-G1.
7. Heiken, G. H. and M. L. Bevier, 1979. Petrology of Tuff Units from the J-13 Drill Site, Jackass Flats, Nevada. LA-7563-MS.
8. Smyth, J. R., 1980 (?) Memo to (?): X-ray Diffraction Analyses of Different Size Fractions, JA-37, -32, and -18.
9. Smyth, J., 1980 (?) Memo to ?: X-ray Diffraction Analyses of J-13 Tuff Samples; Also Size Fractions for YM-5, -30, -42, and -46.
10. Smyth, J., 1980 (?) Memo to (?): X-ray Diffraction Analyses of YM-22; -38, -15, -18, -49, -54, JA-18, -32, -37.
11. Sykes, M. L., G. H. Heiken and J. R. Smyth (1979) Mineralogy and Petrology of Tuff Units from the UF25a-1 Drill Site, Yucca Mountain, Nevada. LA-8139-MS.
12. Vine, G. N. et al., 1980, Radionuclide Transport and Retardation in Tuff. LA-UR-80-2949.
13. Vine, E. N. et al., 1980 Current Status of Laboratory Sorption Studies. LA-UR-80-3357.

Printed in the United States of America
Available from
National Technical Information Service
US Department of Commerce
5285 Port Royal Road
Springfield, VA 22161

Microfiche (A01)

Page Range	NTIS Price Code
001-025	A02
026-050	A03
051-075	A04
076-100	A05
101-125	A06
126-150	A07
151-175	A08
176-200	A09
201-225	A10
226-250	A11
251-275	A12
276-300	A13
301-325	A14
326-350	A15
351-375	A16
376-400	A17
401-425	A18
426-450	A19
451-475	A20
476-500	A21
501-525	A22
526-550	A23
551-575	A24
576-600	A25
601-up*	A99

*Contact NTIS for a price quote.

Los Alamos